

# NAVAL POSTGRADUATE SCHOOL MONTEREY, CALIFORNIA



## THESIS

DTIC QUALITY INSPECTED 2

### TRANSIENT PHENOMENA IN THERMOACOUSTIC PRIME MOVERS

by

Ching-Kai Meng

June, 1996

Thesis Advisor:  
Co-Advisor:

Anthony A. Atchley  
Robert M. Keolian

Approved for public release; distribution is unlimited.

19961001 038

REPORT DOCUMENTATION PAGE			Form Approved OMB No. 0704-0188	
Public reporting burden for this collection of information is estimated to average 1 hour per response, including the time for reviewing instruction, searching existing data sources, gathering and maintaining the data needed, and completing and reviewing the collection of information. Send comments regarding this burden estimate or any other aspect of this collection of information, including suggestions for reducing this burden, to Washington Headquarters Services, Directorate for Information Operations and Reports, 1215 Jefferson Davis Highway, Suite 1204, Arlington, VA 22202-4302, and to the Office of Management and Budget, Paperwork Reduction Project (0704-0188) Washington DC 20503.				
1. AGENCY USE ONLY (Leave blank)	2. REPORT DATE June 1996	3. REPORT TYPE AND DATES COVERED Master's Thesis		
4. TITLE AND SUBTITLE TRANSIENT PHENOMENA IN THERMOACOUSTIC PRIME MOVERS		5. FUNDING NUMBERS		
6. AUTHOR(S) Meng, Ching-Kai				
7. PERFORMING ORGANIZATION NAME(S) AND ADDRESS(ES) Naval Postgraduate School Monterey CA 93943-5000		8. PERFORMING ORGANIZATION REPORT NUMBER		
9. SPONSORING/MONITORING AGENCY NAME(S) AND ADDRESS(ES)		10. SPONSORING/MONITORING AGENCY REPORT NUMBER		
11. SUPPLEMENTARY NOTES The views expressed in this thesis are those of the author and do not reflect the official policy or position of the Department of Defense or the U.S. Government.				
12a. DISTRIBUTION/AVAILABILITY STATEMENT Approved for public release; distribution is unlimited.			12b. DISTRIBUTION CODE	
13. ABSTRACT (maximum 200 words) The purpose of this thesis is to investigate the evolution of the acoustic pressure waveform and temperature change across the heat exchangers as functions of time in a thermoacoustic prime mover. Measurements are reported for both nitrogen and helium gas under different mean pressures and initial temperature differences. Aspects of this thesis included the design and construction of the prime mover and implementation of a computer controlled data acquisition system. Tha goal is to form a set of data with which to test transient, nonlinear theories of thermoacoustics. The main conclusion is that models will have to take into account the performance of heat exchangers to accurately model the initial build up of the oscillations.				
14. SUBJECT TERMS Acoustics; Thermoacoustic; Prime Mover; Transient Phenomena			15. NUMBER OF PAGES 72	
			16. PRICE CODE	
17. SECURITY CLASSIFICATION OF REPORT Unclassified	18. SECURITY CLASSIFICATION OF THIS PAGE Unclassified	19. SECURITY CLASSIFICATION OF ABSTRACT Unclassified	20. LIMITATION OF ABSTRACT UL	

NSN 7540-01-280-5500

Standard Form 298 (Rev. 2-89)  
Prescribed by ANSI Std. Z39-18 298-102



Approved for public release; distribution is unlimited.

**TRANSIENT PHENOMENA IN THERMOACOUSTIC  
PRIME MOVERS**

Meng, Ching-Kai  
Lieutenant Commander, Taiwan Navy  
B.S., Chinese Naval Academy, 1985

Submitted in partial fulfillment of the  
requirements for the degree of



**MASTER OF SCIENCE IN ENGINEERING ACOUSTICS**

from the

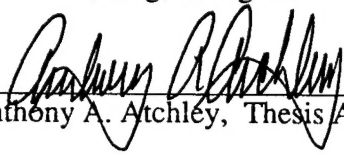
**NAVAL POSTGRADUATE SCHOOL**

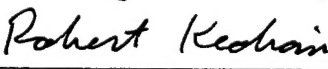
June 1996

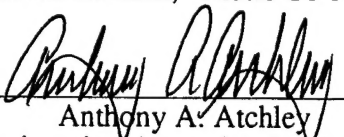
Author:

   
Meng, Ching-Kai

Approved by:

  
Anthony A. Atchley, Thesis Advisor

  
Robert M. Keolian, Thesis Co-Advisor

  
Anthony A. Atchley  
Chairman, Engineering Acoustics Academic Committee



## ABSTRACT

The purpose of this thesis is to investigate the evolution of the acoustic pressure waveform and temperature change across the heat exchangers as functions of time in a thermoacoustic prime mover. Measurements are reported for both nitrogen and helium gas under different mean pressures and initial temperature differences. Aspects of this thesis included the design and construction of the prime mover and implementation of a computer controlled data acquisition system. The goal is to form a set of data with which to test transient, nonlinear theories of thermoacoustics. The main conclusion is that models will have to take into account the performance of heat exchangers to accurately model the initial build up of the oscillations.



## TABLE OF CONTENTS

I. INTRODUCTION .....	1
II. EXPERIMENTAL APPARATUS AND PROCEDURE.....	3
A. INTRODUCTION .....	3
B. EXPERIMENTAL APPARATUS.....	3
1. Stack/Heat Exchanger .....	3
2. Thermocouple flanges .....	4
3. DeltaE.....	9
4. The Primer Mover.....	9
a. Hot End.....	9
b. Cold End .....	12
c. Cold End Insulator .....	12
5. The Temperature Control And Measurement System.....	15
6. Microphone and Mean Gas Pressure .....	15
7. Data Acquisition System. ....	17
C. EXPERIMENTAL PROCEDURE AND DATA ACQUISITION .....	17
III. OBSERVATIONS, RESULTS AND DISCUSSION .....	19
A. REPRESENTATIVE DATA.....	19
1. Nitrogen Data.....	19
2. Helium Data.....	22
B. CALCULATION OF STEADY STATE HEAT FLOW .....	26
IV. SUMMARY AND RECOMMENDATION .....	33



A. SUMMARY .....	33
B. RECOMMENDATION.....	33
APPENDIX A. GRAPHS OF EXPERIMENTAL RESULTS .....	35
APPENDIX B. TEMPERATURE PROFILES .....	51
APPENDIX C. DELTAE INPUT FILE FOR PRIME MOVER DESIGN .....	57
LIST OF REFERENCES .....	61
INITIAL DISTRIBUTION LIST .....	63

## I. INTRODUCTION

There are two basic classes of thermoacoustic engines: heat pumps (or refrigerator) and prime movers (or motors) [Refs. 1-3]. Regardless of which type of device is being considered, a thermoacoustic engine is made up of three major components: an acoustic resonator; heat exchangers; and a porous, poorly thermally conducting structure known as a stack. A thermoacoustic heat pump uses a high amplitude acoustic standing wave to transport (or pump) heat along the boundary of a plate or other suitable structure situated in the standing wave. This acoustically generated heat flow results in a thermal gradient being established across the plate. In other words, acoustic energy is converted into stored thermal energy, which in turn can be used in a number of practical applications. It is also possible to generate sound within a resonator, by forcing a sufficiently large temperature difference across a stack. Such a device, known as a thermoacoustic prime mover, is the subject of this thesis.

Practically all analysis of thermoacoustic engines is based on linear, steady state models. [Refs. 1,4] Therefore, with few exceptions, analysis of transient effects is not possible. One exception is the analysis of the initial buildup of oscillations in a prime mover. The initial growth of oscillations can be well characterized by a single, amplitude independent, time constant that can be predicted from steady state arguments. [Refs. 2,5]

Prosperetti and coworkers have begun to develop a nonlinear, time dependent model of thermoacoustics. [Refs. 6] However, there is a lack of published data with which to compare the results of such a model. Motivated by this lack of data, we have made measurements of the evolution of the acoustic pressure waveform in a prime mover. The purpose of these measurements is to provide set of data to test theoretical predictions.

The data consists of measurements of the acoustic waveform and heat exchanger temperatures as function of time. Two different gases (nitrogen and helium) are used at

various mean gas pressure and initial temperature differences imposed across the stack. The growth rate of harmonics are determined from the waveform.

In Chapter II, we describe the experimental apparatus and procedure, followed by observations, results and discussion in Chap. III. The last chapter will present a summary and recommendations.

## **II. EXPERIMENTAL APPARATUS AND PROCEDURE**

### **A. INTRODUCTION**

A description of the experimental apparatus is given in this chapter, along with a discussion of the procedure followed during data acquisition. Conversations with potential collaborators indicated that they would prefer to model a prime mover that had registered stack plates and heat exchanger fins, i.e. an assembly in which the stack plates and heat exchanger fins are aligned and in good thermal contact. This is not the typical case. However, the stack plates and heat exchanger fins from the original Hofler tube are so aligned. [Refs. 7] Therefore, it was decided to make use of this stack/heat exchanger assembly. Having decided on the stack and heat exchanger, the next task in the design of the prime mover was to determine the position of the stack within the acoustic resonator. We used DeltaE for this purpose.[Ref. 8]

This chapter begins with a description of the stack/heat exchanger assembly. Next we describe how the heat exchangers are instrumented with thermocouples. After that, the computer modeling used to determine the lengths of the hot and cold ends of the prime mover is described. Because we are interested in the build up of oscillations, a method of turning the prime mover on and off is required. The solution to this design criterion is discussed. Having presented all the pertinent details of the prime mover, the complete assembly is described. We next describe the LabVIEW based data acquisition system. The chapter concludes with a discussion of the procedures followed during data acquisition.

### **B. EXPERIMENTAL APPARATUS**

#### **1. Stack/Heat Exchanger**

The stack (shown in Fig. 1) is made using two brass flanges separated by a short length of poorly thermally conducting stainless steel tube and filled with 22 G-10 fiberglass plates, each 0.38 mm thick and spaced from one another by 1.00 mm. The widths of the

plates were cut to conform to the inner diameter of the stainless steel tube. All the fiberglass plates had a common length of 16.5 mm. The end of the fiberglass plates were epoxied to 0.38 mm thick by 1.6 mm long copper strips. The widths of these copper strips were approximately equal to the outer dimension of the brass flange. Short copper spacers were placed between the strips. The strips and spacers were sandwiched between two "D" shaped brass segments. The whole assembly was secured with low melting point solder.

The intent of the original Hofler tube was to operate in atmospheric pressure air. We want to use gas at different pressures. It turned out that there were numerous gas leaks between the copper fins and spacers. There leaks were closed with vacuum sealing wax, although in the end the prime mover was not completely leak free. The leak rate was approximately 1% of mean pressure per 5 minutes when the prime mover was pressurized to approximately 1.5 atm with nitrogen gas. During data acquisition the prime mover was maintained at above atmosphere pressure until just before a data run began. At the completion of a data run (which is accomplished in less than one minute) the prime mover was pumped down to less than 500 Pa and repressurized to above atmosphere pressure prior to the next run.

## **2. Thermocouple flanges**

One of the purposes of this thesis is to measure the temperature of the heat exchangers as functions of time. Three Type-T thermocouples were positioned on or near both the hot and cold heat exchangers for this purpose.

The thermocouples were made from OMEGACLAD 304 stainless steel sheath thermocouple wire. The outer diameter of the sheath is 0.062 inch. The individual thermocouple wires are approximately 0.01 inch in diameter. The sheath is packed with magnesium oxide powder insulation. Short pieces (approximately 10 cm long) of the wire were passed through pieces of 1/8 inch diameter copper tubing, approximately 4 cm in length. The stainless steel sheath was soft soldered to the copper tubing, particular attention being paid to the ends of the copper tubing to ensure a leak tight solder joint.

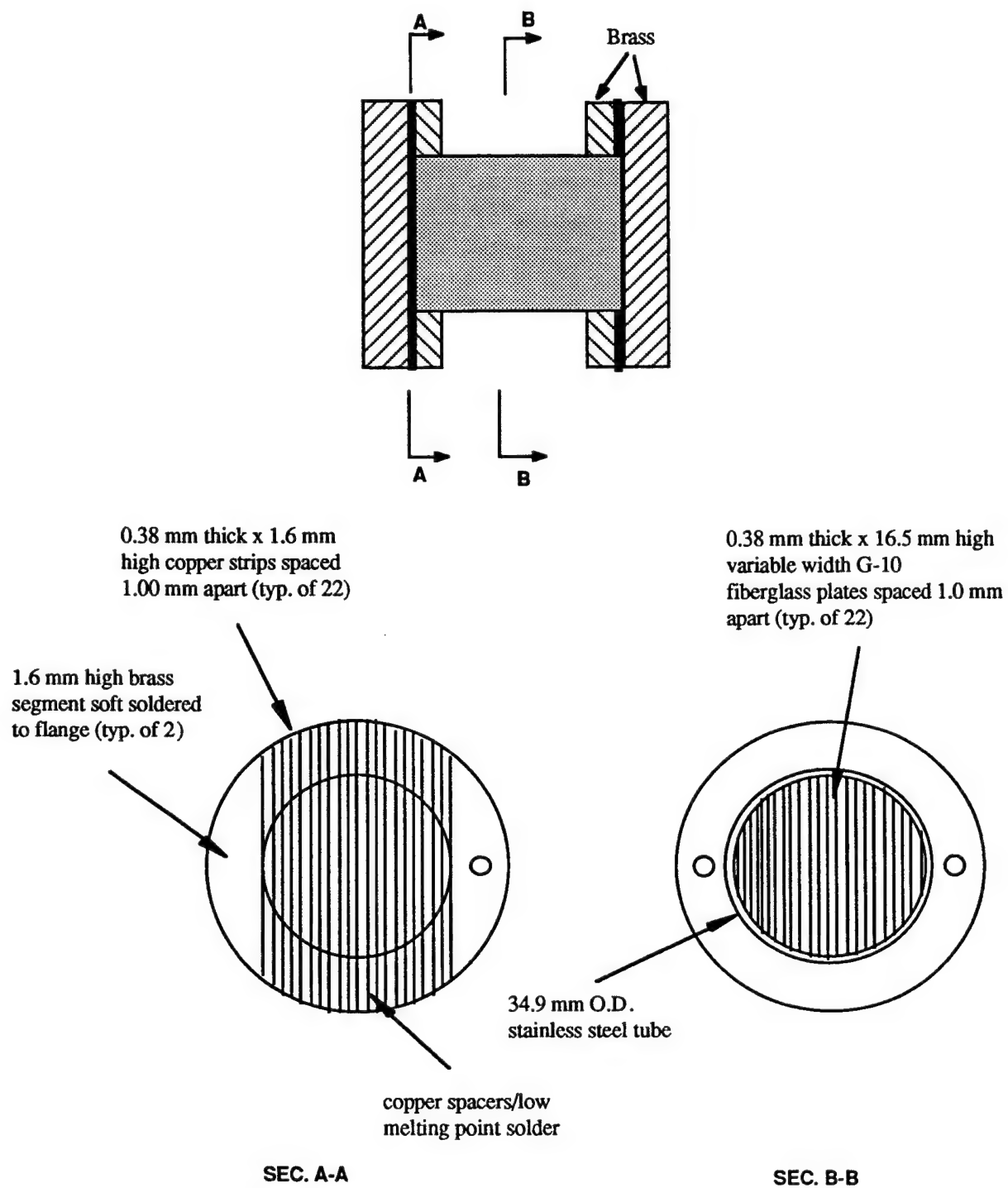


Figure 1 - Drawing of stack/heat exchanger assembly

Next, approximately 1 cm of the sheath was stripped from the ends of the thermocouple wire. The thermocouple wires were fitted through each of three holes drilled through the side of a 0.47 inch thick copper flange. (see Fig. 2) The flange and the three wires were heated on a hot plate. The copper tubing was soldered to the outside of the copper flange with low melting point solder. The stainless steel sheath was soldered to the inside of the flange. After the flange cooled off, thermocouple wires on the inside of the flange were soldered together with soft solder, forming the sensing junction. A small amount of fast-drying epoxy was applied where the thermocouple wires emerged from the sheath to prevent gas leaks through the powder-packed sheath.

Silicone based heat sink compound was applied to the faces of the flanges and the flanges were bolted to the stack flange. At this point two of the thermocouples were soldered to the central heat exchanger fin on both the hot and cold ends. The remaining thermocouple was used to sense the gas temperature. The positions of the thermocouple are described below.

The structure of the hot end thermocouple flange is shown in Fig. 2. The first lead is connected to the edge of the 12th plate about 5.73 mm from the flange's edge. The second lead is connected near the center of the same plate about 15.44 mm from the flange's edge. The last one is exposed to the gas, about 4.33 mm to the closest flange's edge and 3.54 mm above the fin. The hot thermocouple flange also housed two OMEGA Model CIR-1024 cartridge heaters used to maintain the hot end temperature near room temperature.

The same type of thermocouples and feed through were used for the cold end as shown in Fig. 3. One lead is exposed to the gas. The junction is 4.33 mm from the closest edge and 5.42 mm above the fin. The second lead is connected near the center of the 12th fin about 15.44 mm from the flange's edge. The third lead is connected to the edge of the same fin about 4.64 mm from the flange's edge.

Note:

1. Length from the flange's edge to the connection is 5.73 mm.
2. Length from the flange's edge to the connection is 15.36 mm.
3. The distance is 7.26 mm from the closest flange's edge and 3.54 mm above the fin.

Heater

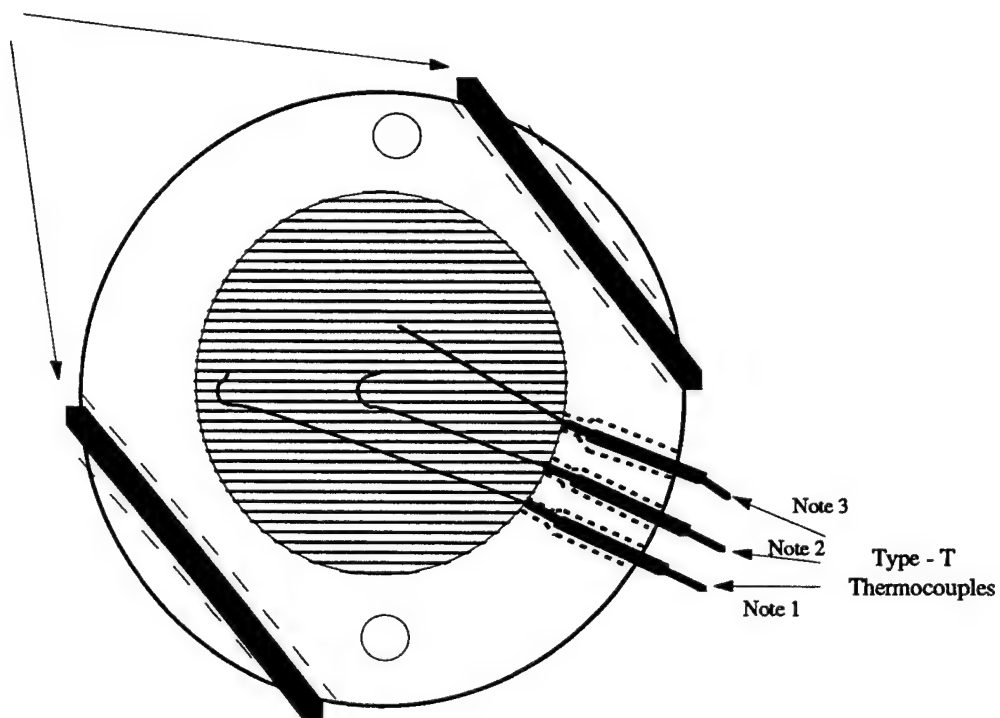
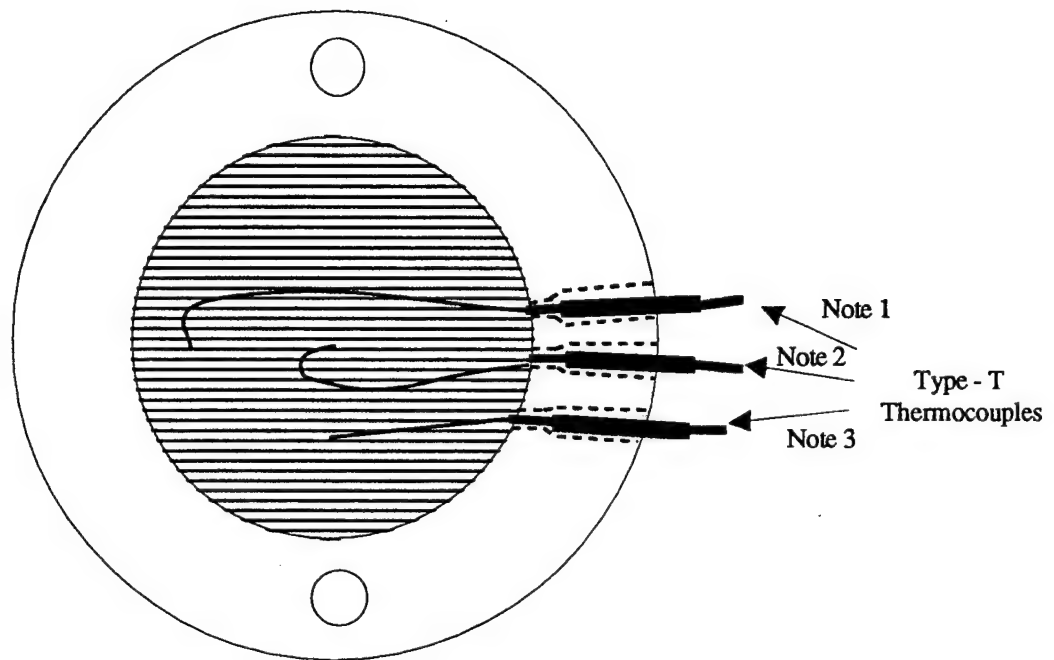


Figure 2 - Hot end thermocouple flange



Note:

1. Length from the flange edge to the connection is 4.64 mm.
2. Length from the flange edge to the connection is 15.44 mm.
3. The distance is 4.33 mm from the closest flange's edge and 5.42 mm above the fin.



**Figure 3 - Cold end thermocouple flange**

### **3. DeltaE**

Having decided on the stack and heat exchanger, it remained to determine the position of the stack within the resonator. In this experiment, the goal is to keep the hot end at room temperature (approximately 293 K) and let the cold end temperature be adjustable. DeltaE was used to model the prime mover in order to determine the lengths of hot and cold ends that give the lowest temperature difference for onset.

DeltaE (Design Environment for Linear Thermoacoustic Engines) is a computer program for modeling and designing thermoacoustic engines and other one-dimensional acoustic apparatus [Ref. 8]. The input file for our prime mover is shown in Appendix C. DeltaE is not designed to find onset conditions. Therefore, we instead found the lowest heat input that gave stable solutions for the prime mover filled with nitrogen gas at 1 atm. mean pressure. This heat input was approximately 20 W. Using this power we varied the cold end length from 10 cm to 20 cm and the hot end length from 30 cm to 60 cm. The results are shown in Fig. 4. This graph shows the steady state temperature difference as function of hot and cold end lengths. The lowest onset conditions occur for cold lengths from about 12 to 16 cm and hot end lengths from about 50 to 60 cm. The lowest temperature difference happened at cold end approximately 13 cm and hot end 55 cm long, indicated by the star in Fig. 4.

### **4. The Primer Mover**

In this section, we will describe the structure of the prime mover based on the results from DeltaE. The overall assembly is shown in Fig. 5.

#### ***a. Hot End***

The results of the DeltaE analysis of the prime mover indicated that the length of the hot end should be approximately 13 cm, from the rigid end to the hot heat exchanger fin. Referring to Fig. 6 the hot end consists of a 1.375 OD, 1.25 ID, 3.15 inch long copper tube. A copper flange was hard soldered to one end of the tube. This flange

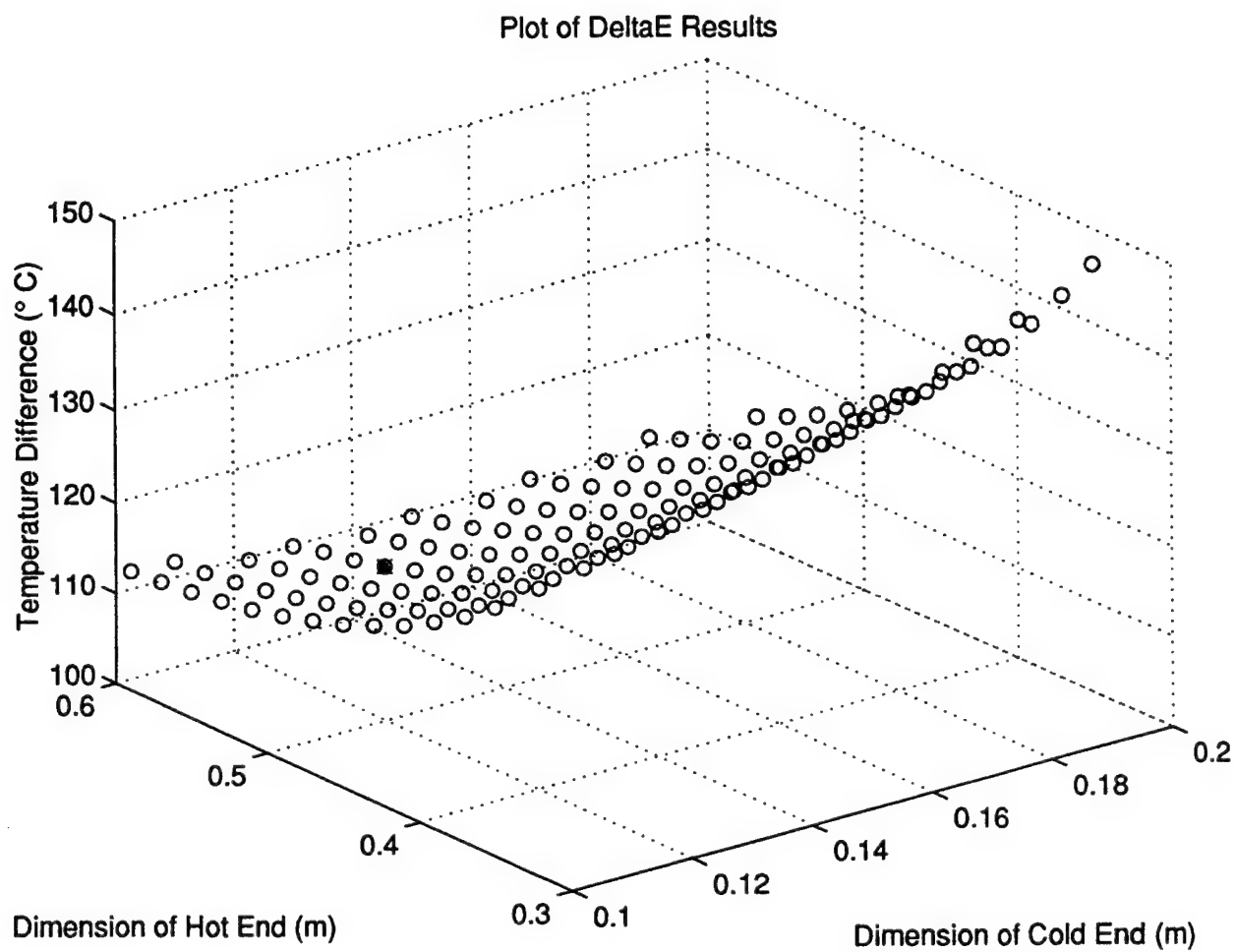


**Figure 4 - Results of DeltaE output to determine prime mover dimensions**

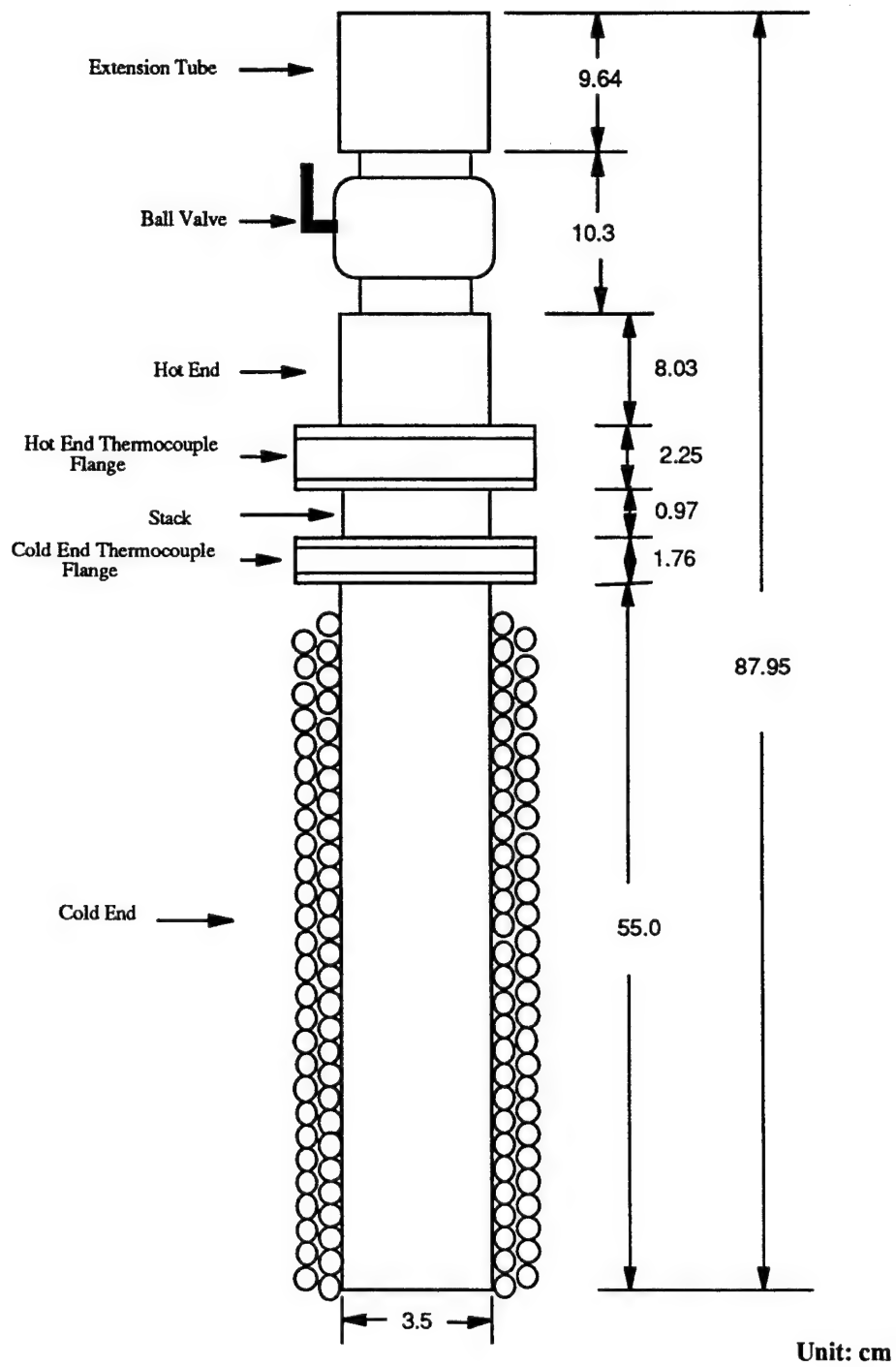


Figure 5 - Prime mover configuration

allowed for connecting the hot end to the thermocouple flange and stack. An off-the-shelf, male pipe copper coupler was soft soldered to the other end. A one inch ball valve was screwed onto the coupler. The ball valve was designed for use with natural gas lines. A 3.8 inch copper extension tube is connected to the other side of the valve. A copper end cap is soldered to the tube. The end cap is drilled and tapped to accommodate a gas fill tube.

The purpose of ball valve is to turn the prime mover on and off. With the ball valve closed, the stack is in a thermoacoustically-efficient position. The ball effectively formed the rigid end of the prime mover. With the ball open the stack is no longer in the proper place and so oscillations cease.

The effective length of the hot end was determined by closing the ball valve and filling the tube with water. It required 89.0 ml of water to fill the tube. This volume is equivalent to a 11.24 cm long, 3.175 cm ID tube.

#### ***b. Cold End***

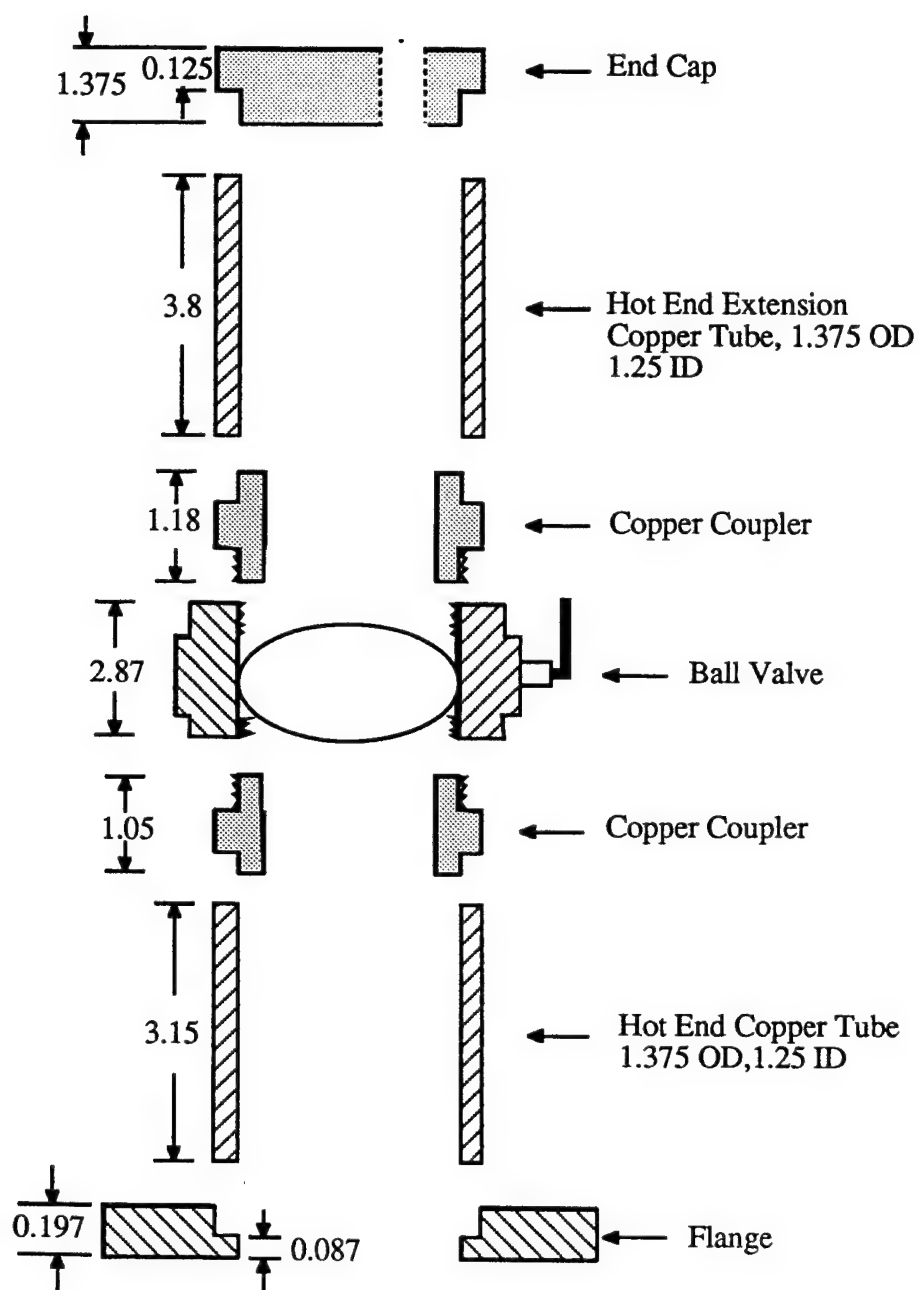
The results of the DeltaE analysis indicated that the length of the cold end should be approximately 55 cm long, from the rigid end to the cold heat exchanger. A 3.175 cm ID copper tube was fitted with a copper end cap and a copper flange (identical to the one on the hot end) as shown in Fig. 7. The internal length of the cold end duct is 54.4 cm.

The outside of the cold end duct was wrapped with two layers of 1/4 inch soft copper tubing. The tubing was soft soldered to the cold end duct. Cold nitrogen gas is circulated through the tubing to cool the cold end, as described below.

#### ***c. Cold End Insulator***

We want to be able to maintain a uniform temperature along the cold end for temperatures down to that of liquid nitrogen. We also need to provide support for the prime mover. The cold end insulator provides for both.

The insulator consisted of a 24 inch long, 12 inch diameter PVC pipe glued to a 1 inch thick PVC base. The pipe and base were cut in half along the long axis of the



Unit : inch

Figure 6 - Hot end configuration

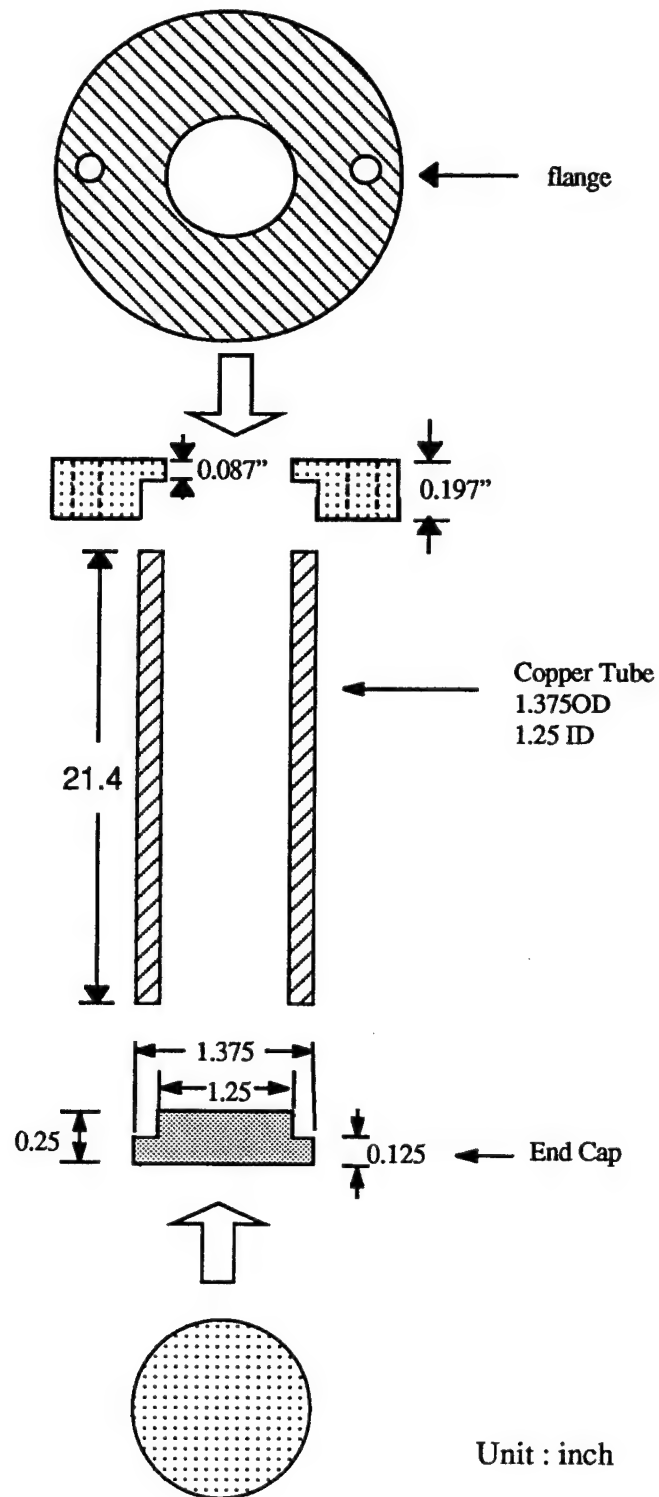


Figure 7 - Cold end configuration

tube and hinged along one side. The two halves were isolated from one another by two pieces of thin plastic sheet. The prime mover was placed between the plastic sheet and the pipe was filled with expanding foam, similar to that used in packing boxes.

### **5. The Temperature Control And Measurement System**

The temperature of the hot end was maintained near room temperature by means of two Omega Model CIR-1024 cartridge heaters inserted into the hot thermocouple flange. Thermal contact between the cartridge and flange is enhanced with silicone heat sink compound. As shown in Fig. 8, the temperature of hot end flange is sensed by a Type-T thermocouple connected to an autotuning Omega Engineering Model CN9000A series Temperature Controller. The set point temperature was 25° C. The controller generates a DC control voltage which is amplified with a TECHRON 5530 power supply amplifier and sent to the heaters.

In addition to the six heat exchanger thermocouples, five more were attached to the outside of the prime mover. Three were located at the bottom, center, and flange of the cold end. One was on the hot end flange. The last thermocouple was located on the hot end near the ball valve. The outputs from all eleven thermocouples were sent to a KEITHLEY Model 740 System Scanning Thermometer coupled to a KEITHLEY Model 705 Scanner. The internal cards were KEITHLEY Models 7402 and 7057A.

The cold end temperature was controlled by circulating cold nitrogen gas through the copper tubing wrapped around the cold end. Nitrogen gas from a standard size cylinder was forced through a coil of copper tubing submerged in a liquid nitrogen filled Dewar. The tubing was connected to that wrapped around the cold end. By adjusting the flow rate of the gas the cold end temperature could be set to any temperature down to approximately -190° C. The uniformity of the cold end temperature is indicated in Appendix B.

### **6. Microphone and Mean Gas Pressure**

The acoustic signal is detected by an ENDEVCO model 8530C-15 piezoresistive absolute pressure transducer located in the coupler near the ball valve. The sensitivity of the



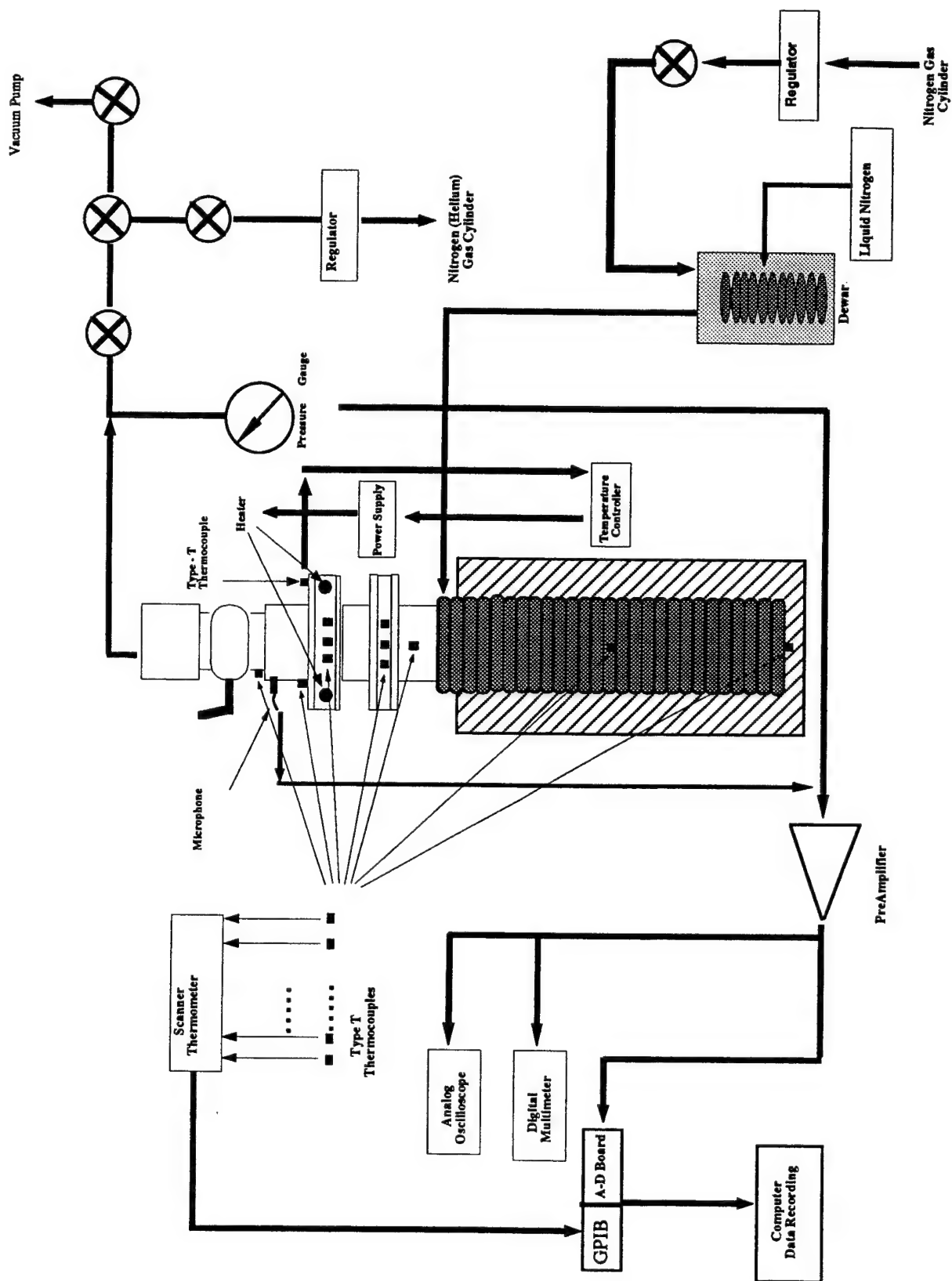


Figure 8 - Schematic diagram of the instrumentation used in the experiment

transducer is 13.60 mv/psi and excitation is 10 Vdc. The output signal from the transducer is amplified by a differential amplifier and then sent to a Kikusui COS6100A oscilloscope for signal displaying. The signal is also sent to the A-D board. The mean gas pressure was measured with an OMEGA Model PX304-300AV pressure transducer. The transducer was connected to the gas fill lines.

## **7. Data Acquisition System**

The amplified microphone output and the six heat exchanger thermocouple signal were sent to a National Instruments Model PCI-MIO E A/D board. The thermocouple signals were taken directly from the KEITHLEY 7402 Thermocouple boards through copper wires. These seven signals were digitalize and stored via a LabVIEW program running on a Power Macintosh 7200/90. The KEITHLEY Thermometer and Scanner were read via the GPIB bus. The voltage data from the thermocouples were converted to temperatures using the following procedure. During the initial and final scans of temperatures from the KEITHLEY Thermometer, the temperature of the on-card isothermal connector block was recorded. This reference temperature was converted to a reference voltage using the Seebeck coefficient at normal room temperature. This voltage is referenced to 0° C. The thermocouple voltages read by the A/D board were added to this reference voltage. This total voltage was converted to a temperature using a 7th order polynomial. The coefficients for polynomial were taken from the OMEGA Temperature reference information.

## **C. EXPERIMENTAL PROCEDURE AND DATA ACQUISITION**

The hot end of the prime mover was maintained at approximately 25° C by using the temperature controller. The temperature at the cold end could be varied continuously from 25° C to -190° C. First, we used the vacuum pump to pump out the gas inside the prime mover to less than 500 Pa. Then the prime mover was filled with nitrogen or helium. The process was repeated several times to make sure that the gas inside the prime mover is

pure. Once the prime mover was filled, we cooled down the cold end by circulating cold nitrogen gas. When the prime mover reached the desired temperature difference the ball valve was closed to start the oscillations.

There are three steps to data acquisition. Step one was to scan all thermocouple channels using the GPIB bus before closing the ball valve. Next the valve was closed and LabVIEW was used to record the seven data channels. After the valve was opened again, the outputs of all eleven thermocouples were read again. The mean gas pressure was recorded at the same time the temperature scans were made to determine the amount of gas leak. We use different mean pressure and gases (nitrogen and helium), and various temperature differences.

### III. OBSERVATIONS, RESULTS AND DISCUSSION

The primary goal of this experiment is to measure the evolution of the acoustic waveform and the change in temperature across the hot and cold heat exchangers as oscillations built up to steady state. The variable parameters are gas type, mean gas pressure, and temperature difference imposed across the stack. As was mentioned in the previous chapter, we used LabVIEW to digitize and store data via GPIB and an A/D board. Matlab was used to further process the data. In this chapter, we present results for a two representative conditions. A more complete set of results is shown in Appendix A. Temperature readings from all the thermocouples recorded before and after waveform capture are given in Appendix B. This chapter is divided into two sections. In section A, we will present representative data. In section B, we present an analysis of the heat flow through the stack based on the measured heat exchanger temperatures.

#### A. REPRESENTATIVE DATA

In this section, we discuss two examples of the data: one for nitrogen and another for helium.

##### 1. Nitrogen Data

The first case to be discussed is for the prime mover filled with nitrogen at a mean pressure 104.9 kPa and imposed temperature difference of approximately 160° C, prior to buildup of oscillations. As explained in Chapter II, the mean gap between two stack plates is 0.62 mm. The thermal penetration depth in nitrogen is 0.202 mm at 293 K, 104.9 kPa and 160 Hz. Therefore, the ratio of gap to penetration depth is 3.07. The microphone output and six heat exchanger temperatures were digitized at a sample frequency of 1500 Hz (per channel) for 15 seconds. The voltage data is processed with Matlab to generate temperature and pressure amplitude. The processed data are shown in Fig. 9. The top figure shows the temperature change in hot heat exchanger vs. time, the middle figure

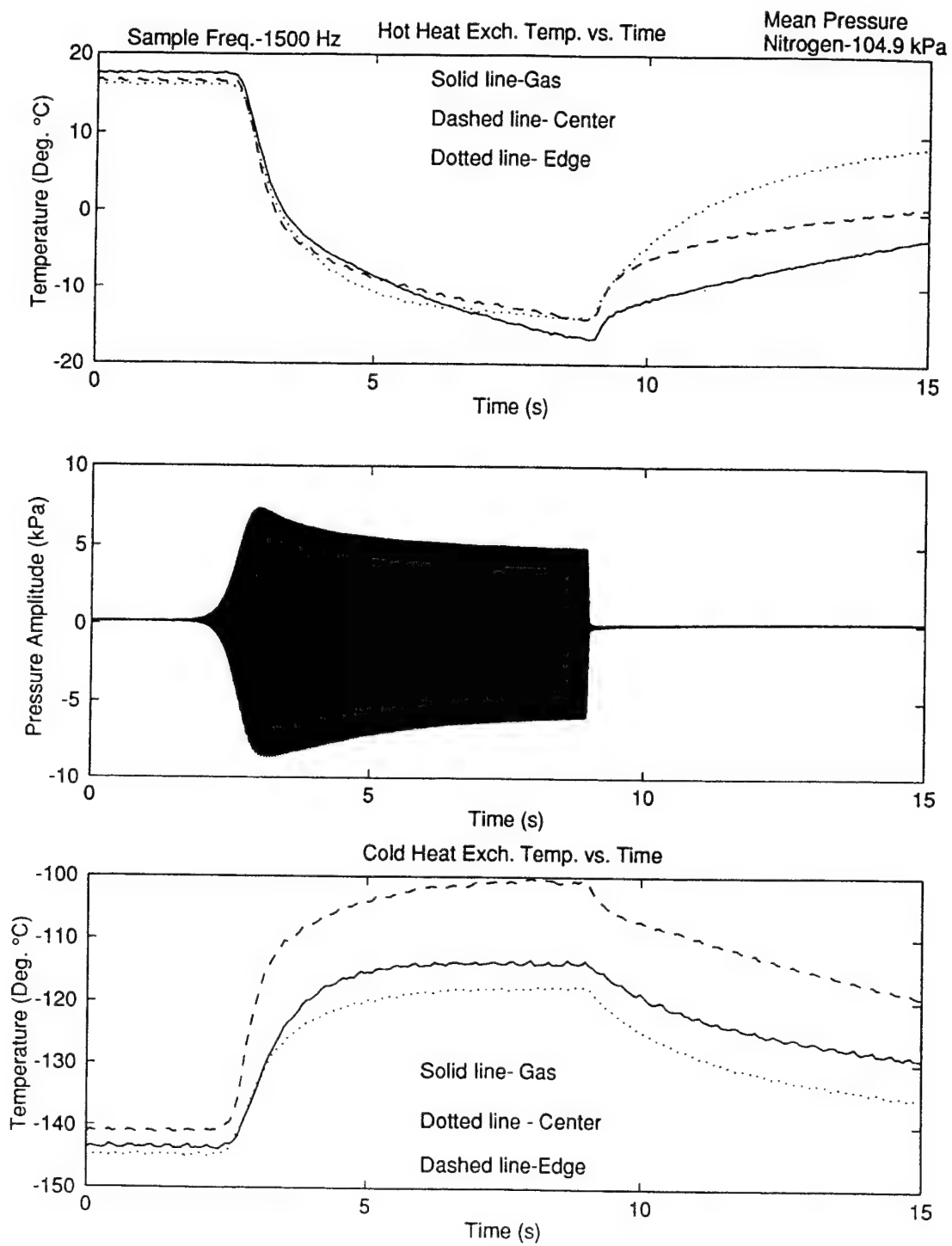


Figure 9 - Results from data run 20

presents the pressure amplitude vs. time, and the bottom figure indicates the temperature change of the cold heat exchanger vs. time. The zero in time has no significance.

The general trend in the data is a smooth buildup in the amplitude of the oscillations, an overshoot, and then a gradual decrease in amplitude to steady state. The valve was closed at approximately 9 seconds, indicated by the rapid quenching of oscillations. We suspect the reason for the overshoot is linked to the evolution in the temperature gradient in the stack. Before the valve is closed, the temperature gradient in the stack is determined by ordinary heat conduction through the stack and surrounding gas. As soon as the amplitude begins to build up, the temperature gradient changes, being determined by thermoacoustic heat transport. As the oscillation grows, the acoustic heat transport becomes dominant and the temperature profile in the stack changes. At the same time, the heat load placed on the heat exchanger increases, being proportional to pressure amplitude squared. At some point the rate at which heat is drawn from (or delivered to) the heat exchangers exceeds the rate at which heat can be supplied to (or removed from) the fin through the flange. At this point the temperature of the heat exchanger changes - the hot heat exchanger becomes cooler and the cold heat exchanger becomes warmer. As can be seen from Fig. 9, the steady state hot heat exchanger temperature is approximately 30° C lower than the initial value, while that of the cold heat exchanger is approximately 30 to 40° C higher.

This change in temperature is no doubt enhanced by the design of the heat exchanger. One would not use this design in a practical device, where it would be important to keep temperature defects to a minimum. However, this type of behavior will still be present, even if to a lesser extent.

It is seen that the prediction of the initial evolution of the pressure amplitude is tied to a prediction of heat exchanger temperature. Successful transient models will have to be able to take this into account.

A one second segment of the data shown in Fig. 9 is displayed in Fig. 10. It is seen that the heat exchanger temperatures are relatively constant until the acoustic pressure reaches approximately 4 kPa peak amplitude.

The data point to a problem with either the heat exchangers or the temperature measurement. This problem is particularly evident in the cold heat exchanger. One would expect that the edge temperature would remain lower than that at the center. However, this is not the case. This result could be explained by poor thermal contact between the fin and the flange. The observation of leaks between the fins and spacers also indicates poor contact. Looking at the hot heat exchanger temperatures, at steady state the edge and center temperature are approximately equal. This indicates there is very little heat flow into the end of the fin where the thermocouple is located. This conclusion is also consistent with the technique used to construct the stack, as discussed in Chapter II. Thermal contact between fins is made through copper spacers. The thermal resistance between different joints is likely to vary. The cumulative thermal resistance between the central fin and the solid brass part of the flanges could be high. The design of a better stack with registered heat exchanger fins is a topic for further work.

The power spectral density of the acoustic pressure from Fig. 9 is shown in Fig. 11. Using this information, we designed an IIR (Infinite Impulse Response) bandpass filter with Matlab - using a 6th order Chebyshev type I filter with 0.5 dB ripple. We used three different passbands 140 to 180 Hz, 300 to 340 Hz, and 460 to 490 Hz to filter the waveform. The positive envelopes of the filtered waveform are presented in Fig. 12. The individual envelopes were produced by taking the magnitude of the sum of the filtered waveform and its Hilbert transform. The graphs show the growth of the first three harmonics of the acoustic signal.

## **2. Helium Data**

In this case, the prime mover was filled with helium at a mean pressure of 54.45 kPa. The thermal penetration depth in helium is 0.585 mm at 54.45 kPa, 293 K and 300

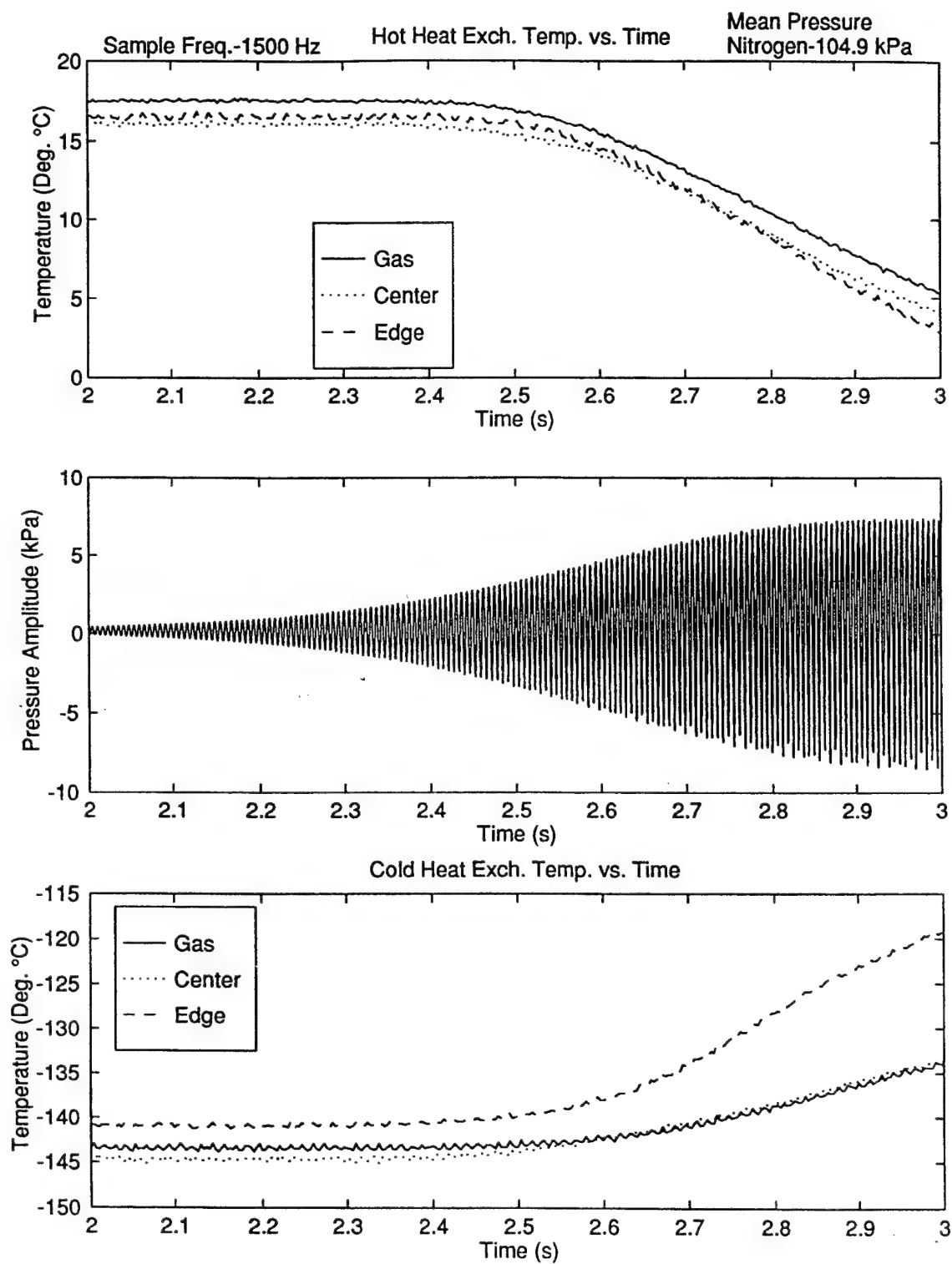
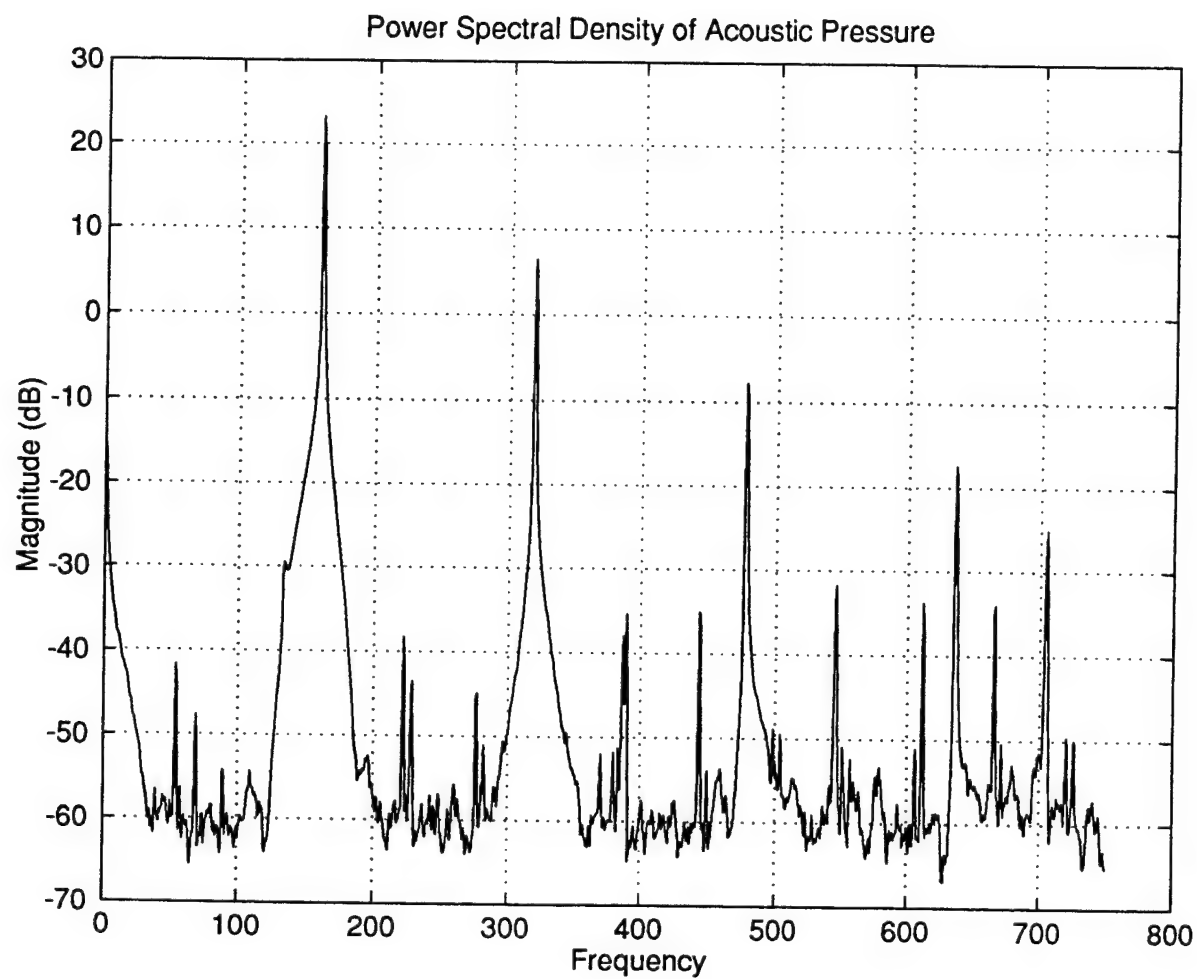


Figure 10 - Results from data run 20





**Figure 11 - Power spectral density of the waveform from Fig. 9**

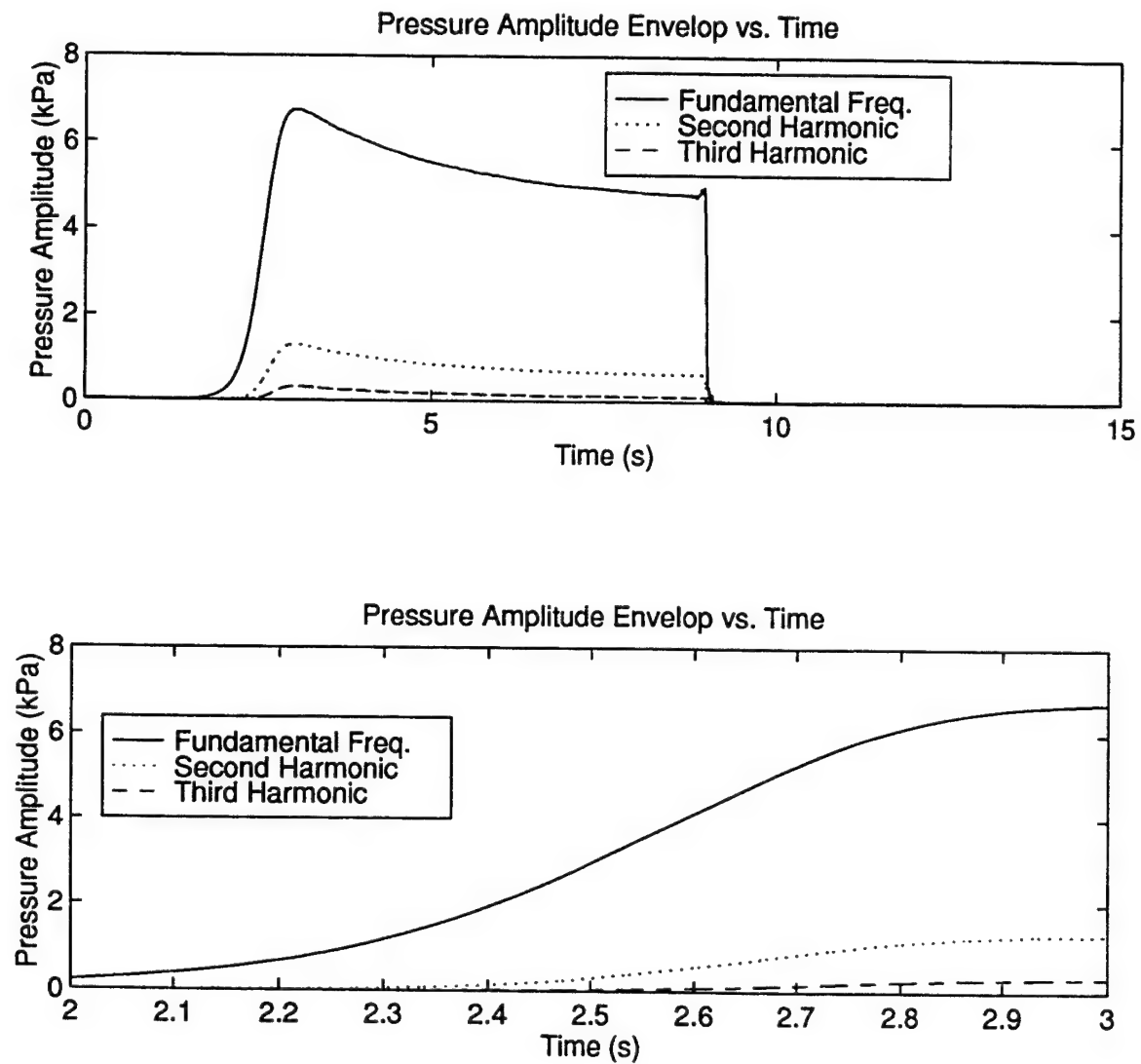


Figure 12 - Graph of Amplitude of the first three harmonics of the waveform from Fig. 9

Hz. Therefore, the ratio of plate spacing to penetration depth is 1.24. Fig. 13 shows experimental results for an initial temperature difference of approximately 170° C, which is well into onset for these conditions. It can be seen that the pressure amplitude builds up very quickly. The 'overshoot' is not so obvious as in the nitrogen case although it is still there. Figure 14 shows the steady state waveform recorded at a sample frequency of 6000 Hz. The waveform is much more distorted than in the nitrogen case. We again used the Chebyshev type I bandpass filter in order to see the harmonic level, shown in Fig. 14 (b). In this case, we used a fourth order Chebychev I filter and four different passbands 250 to 450 Hz, 600 to 750 Hz, 900 to 1100 Hz, and 1250 to 1450 Hz. The power spectral density of acoustic pressure amplitude is also plotted in Fig. 14 (c). The frequency range could have been extended to 3000 Hz. However, we can see from Fig. 14 (b), the amplitudes of harmonics higher than the fourth are very small. Therefore, we only show the first four harmonics levels at steady state.

## B. CALCULATION OF STEADY STATE HEAT FLOW

The heat exchanger temperature measurements can be used to make a simple estimate of the steady state heat flows into and out the heat exchangers. The calculation is based on the heat flow scheme depicted in Fig. 15. The upper part of this figure shows an amount of heat power  $\dot{Q}_h$  entering the ends of one of the hot heat exchanger fins. It is assumed that thermal conduction and acoustic heat transport result in a uniform heat (power) per unit length  $\dot{q}_h$  being transported out of the fin and down the stack plate. At the cold heat exchanger a uniform heat power per unit length  $\dot{q}_c$  flows into the fin. The heat that enters the cold heat exchanger fin flows out through the ends resulting in a heat power flow  $\dot{Q}_c$  exiting the fin.

Consider the heat flow into and out of a small segment of fin of length  $dx$ . Assuming that the temperature of the segment is constant, then the heat outflow must equal the heat inflow. Therefore,

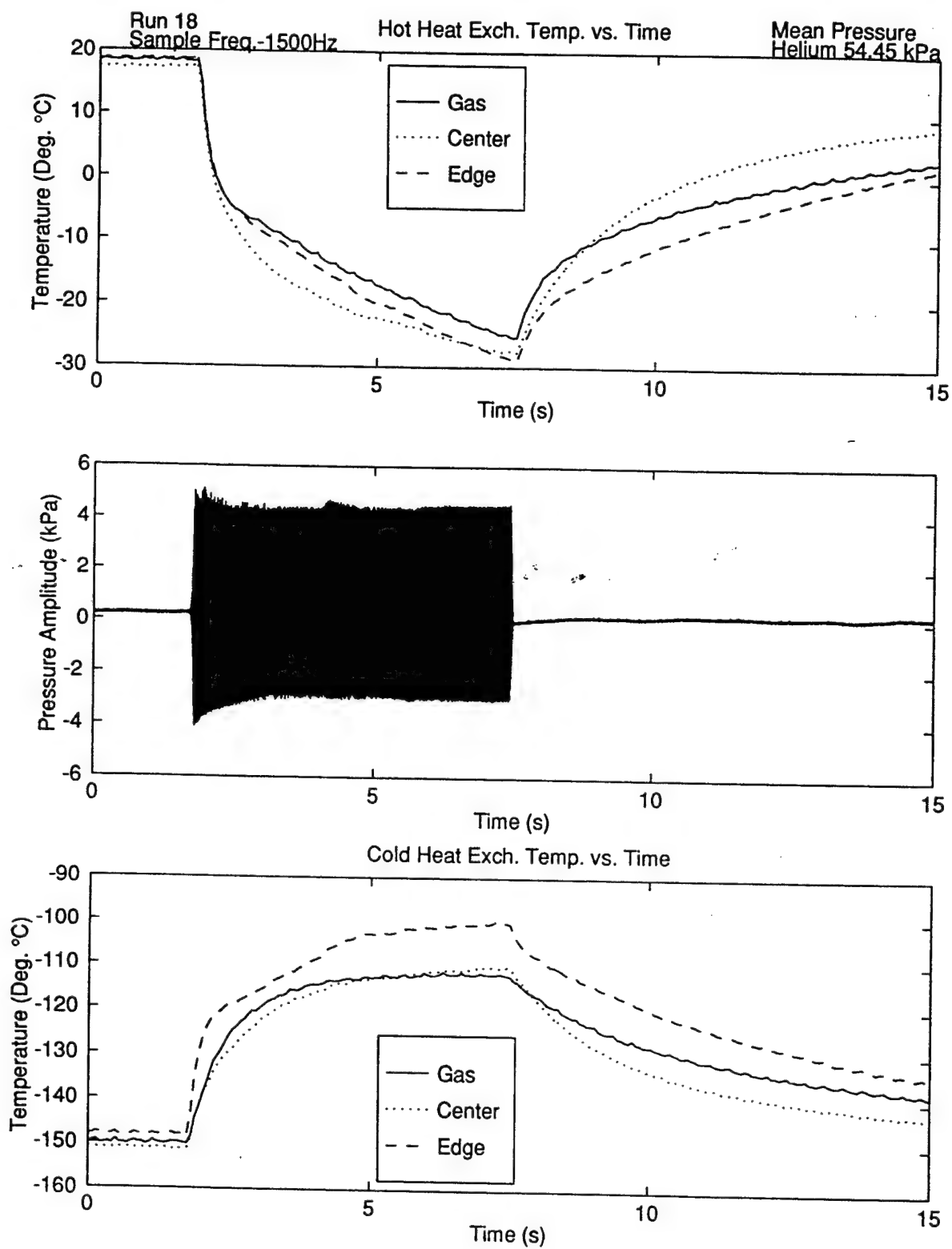
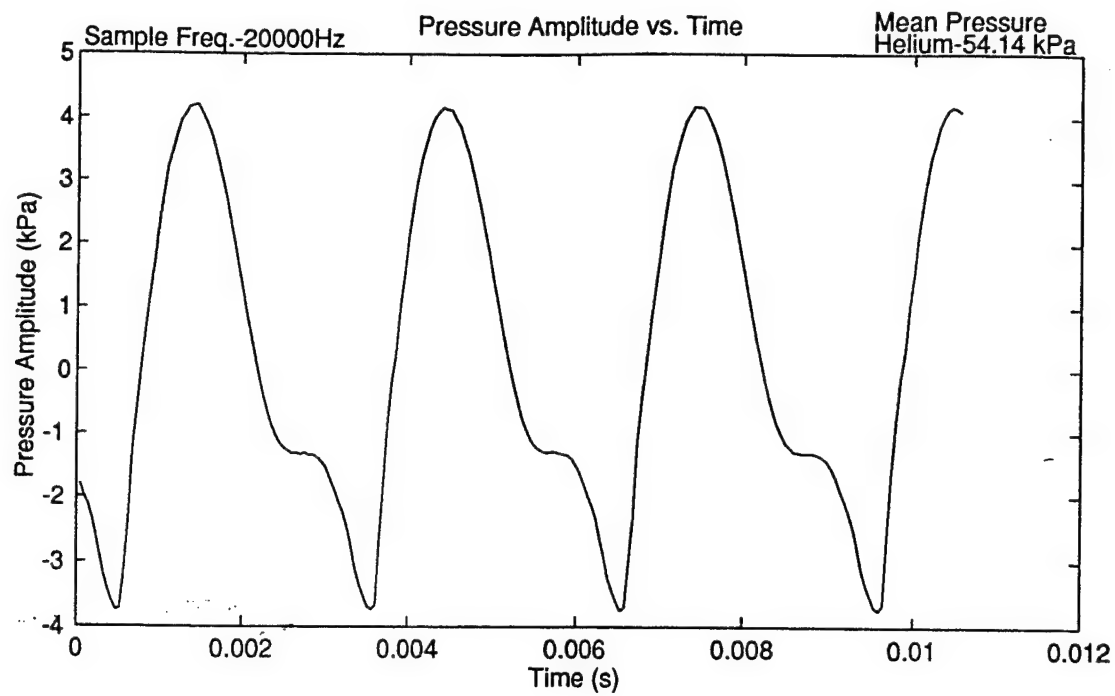
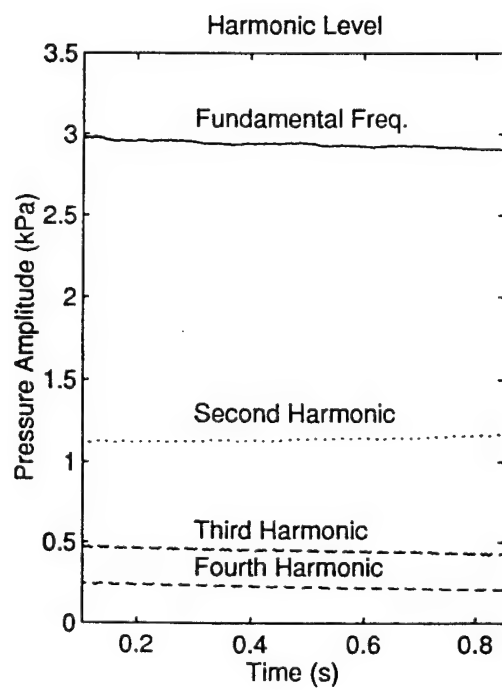


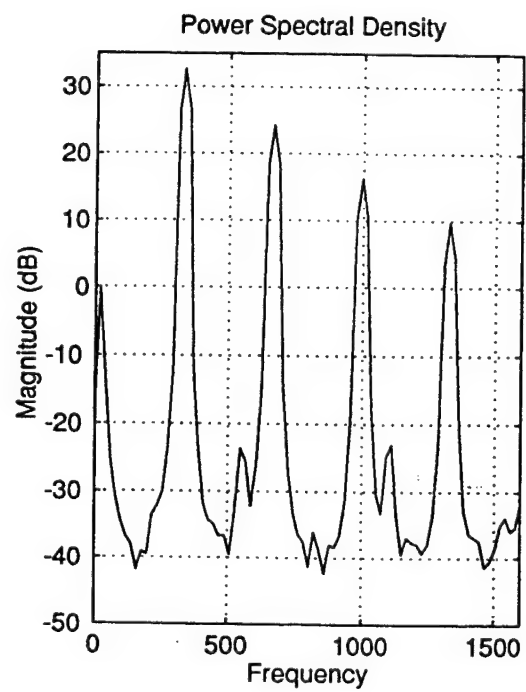
Figure 13 - Results from data run 18



(a)



(b)



(c)

Figure 14 - Steady state waveform for helium

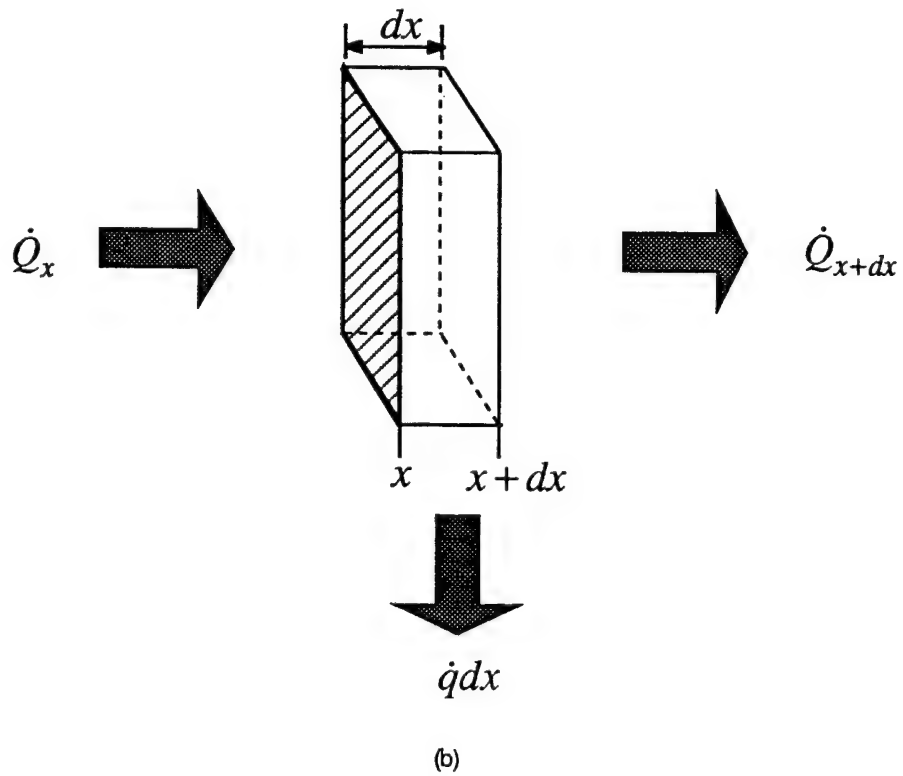
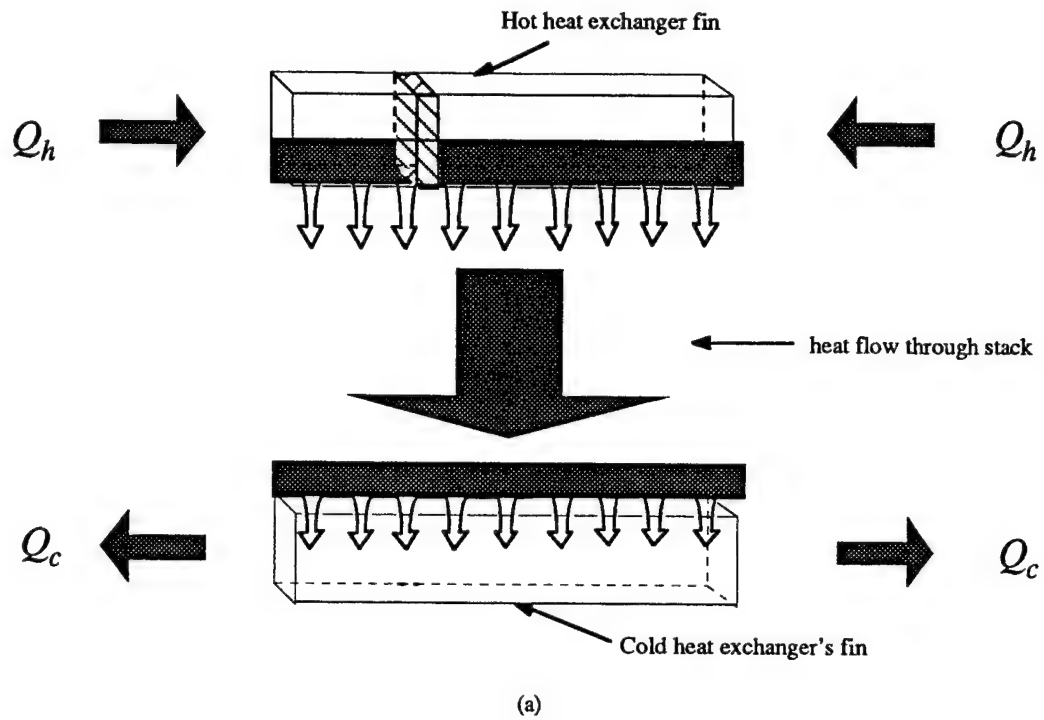


Figure 15 - Heat flow chart

$$\dot{Q}_{x+dx} - \dot{Q}_x = \dot{q}dx. \quad (1)$$

The heat flows at  $x$  and  $x+dx$  are given by the law of conduction to be

$$\dot{Q}_x = -KA\nabla T(x), \quad (2)$$

and

$$\dot{Q}_{x+dx} = -KA\nabla T(x+dx). \quad (3)$$

The temperature gradient at  $x+dx$  is related to that at  $x$  through a Taylor Series,

$$\nabla T(x+dx) = \nabla T(x) + \frac{d\nabla T(x)}{dx}dx + \frac{1}{2} \frac{d^2\nabla T(x)}{dx^2}dx^2 + \dots \quad (4)$$

In the limit of small  $dx$ , this series is well approximated by the first two terms. Substituting Eq. (2) and (3) into Eq. (1) and rearranging gives

$$\frac{d^2T}{dx^2} = \frac{-\dot{q}}{KA}. \quad (5)$$

If it is assume that the right-hand side is independent of  $x$ , Eq. (5) can be easily integrated to find the fin temperature as a function of  $x$ , under the assumption of a uniform heat flow per length exiting the fin. Integrating Eq. (5) once with respect to  $x$  gives

$$\frac{dT}{dx} = -\frac{\dot{q}}{KA}x + C_1. \quad (6)$$

Integrating a second time with respect to  $x$  gives

$$T(x) = -\frac{1}{2} \frac{\dot{q}}{KA}x^2 + C_1x + C_2 \quad (7)$$

Three boundary conditions are sufficient to determine  $\dot{q}$ . Multiplying  $\dot{q}$  by the total length of heat exchanger fins gives  $\dot{Q}$ . Two of the conditions are the measured temperatures at known locations. The third condition is that the temperature gradient must be zero at the center of the fin.

$$\left. \frac{\partial T}{\partial x} \right|_{x=\text{center}} = 0. \quad (8)$$

It is convenient to measure distance from the center of the fin. Applying Eq. (8) to Eq. (6) yields  $C_1=0$ . Using the measured temperature near the edge and center,  $T(x_e)$  and  $T(x_c)$ , and solving for  $\dot{q}$  from Eq. (7) gives

$$\dot{q} = -\frac{KA}{2} \frac{T(x_e) - T(x_c)}{x_e^2 - x_c^2}. \quad (9)$$

The total heat flow  $\dot{Q}$  is therefore given by

$$\dot{Q} = -\frac{KAL_f}{2} \frac{T(x_e) - T(x_c)}{x_e^2 - x_c^2}. \quad (10)$$

where  $L_f$  is the total length of heat exchanger fin for all the plates.

The calculated heat flows for Run 18 and 20 are shown in the table below. The total fin length for our stack is 0.648 cm.

	T(edge) Cold end	T(center) Cold end	T(edge) Hot end	T(center) Hot end	$\dot{Q}_c$	$\dot{Q}_h$
Run18 (Helium)	-99.8° C	-110.2° C	-29° C	-27.75° C	21.71 W	3.15 W
Run20 (Nitrogen)	-100.2° C	-117.4° C	16.7° C	14.1° C	35.95 W	6.54 W

The discrepancy between the values for  $\dot{Q}_c$  and  $\dot{Q}_h$  is unreasonable. This discrepancy also points to a flaw in the heat exchanger design. This conclusion was discussed earlier when the evolution of the heat exchanger temperature was considered.





## **IV. SUMMARY AND RECOMMENDATION**

### **A. SUMMARY**

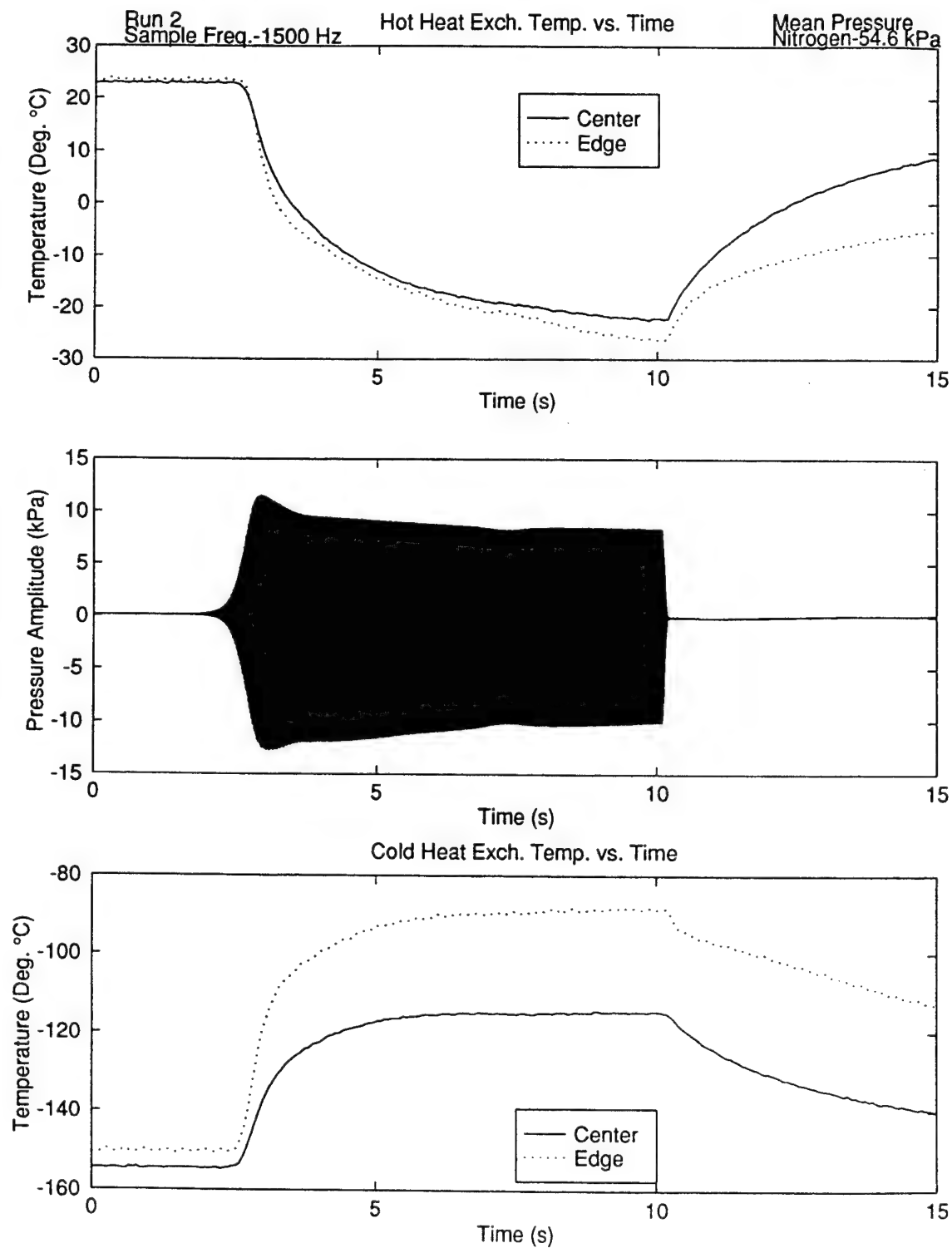
The purpose of this thesis was to investigate the evolution of the acoustic pressure waveform and temperature change across the heat exchangers as functions of time in a thermoacoustic prime mover. Measurements were made with both nitrogen and helium gas under different mean pressures and initial temperature difference. Aspects of this thesis included the design and construction of the prime mover and implementation of a computer controlled data acquisition system. The goal is to form a set of data with which to test transient, nonlinear theories of thermoacoustics. The main conclusion is that models will have to take into account the performance of heat exchangers to accurately model the initial build up of oscillations.

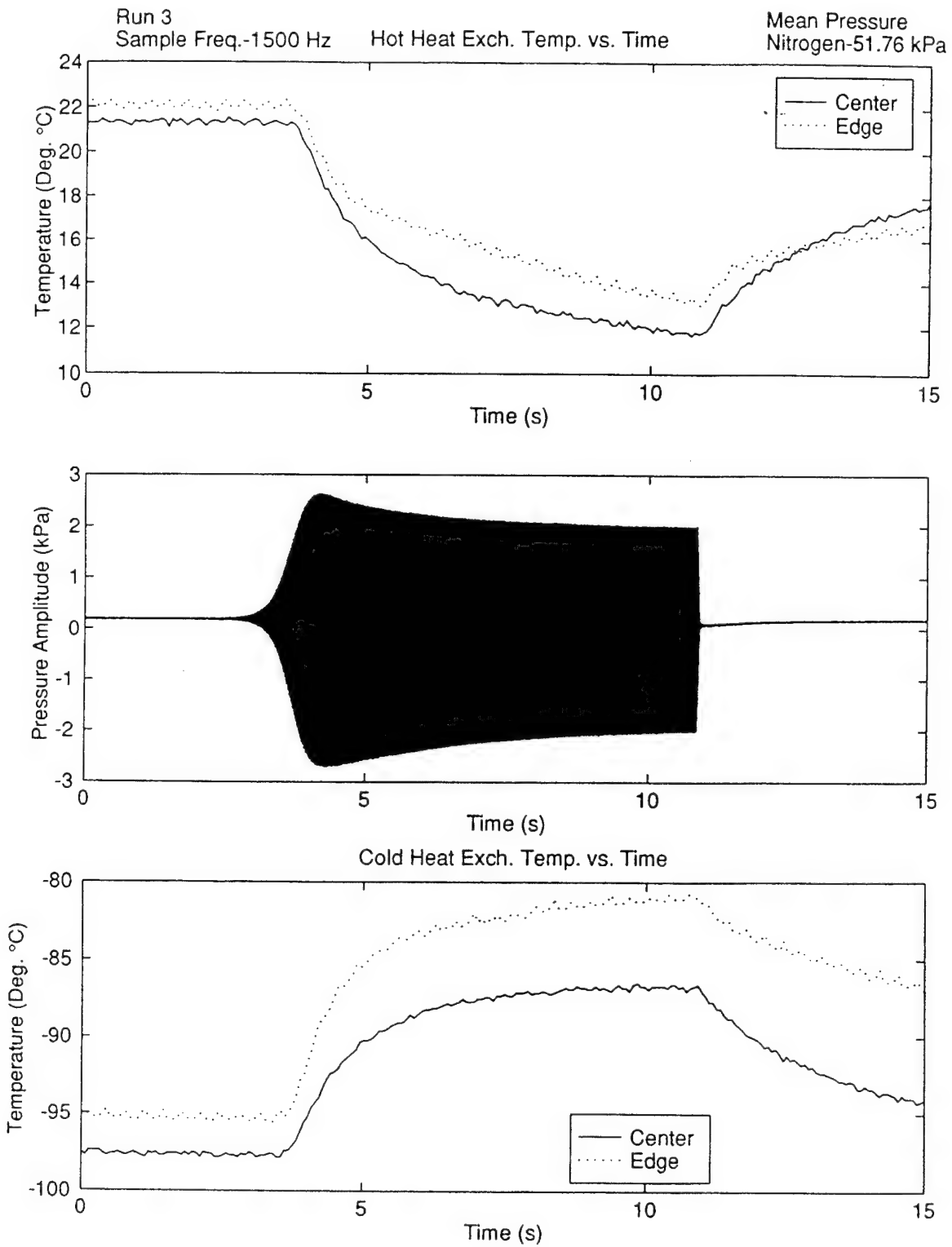
### **B. RECOMMENDATION**

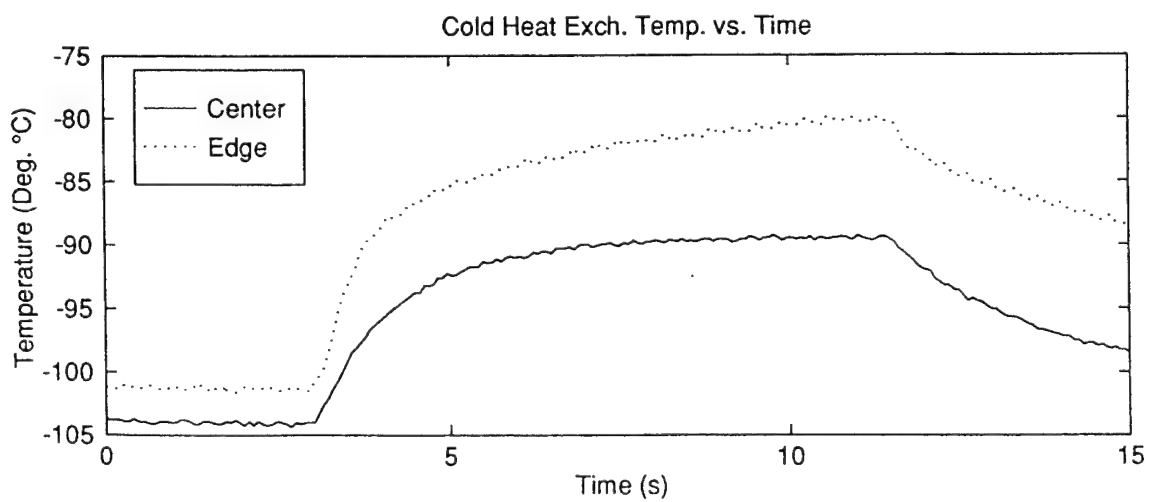
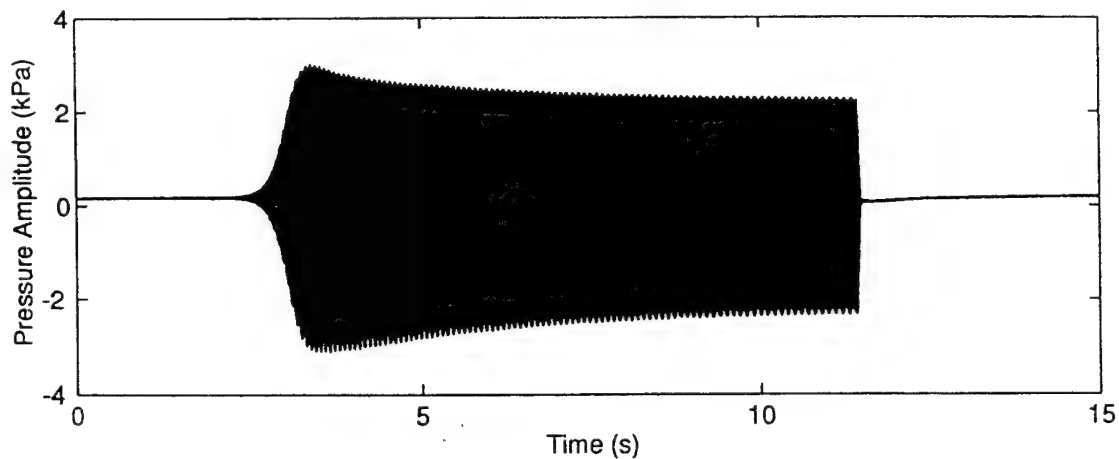
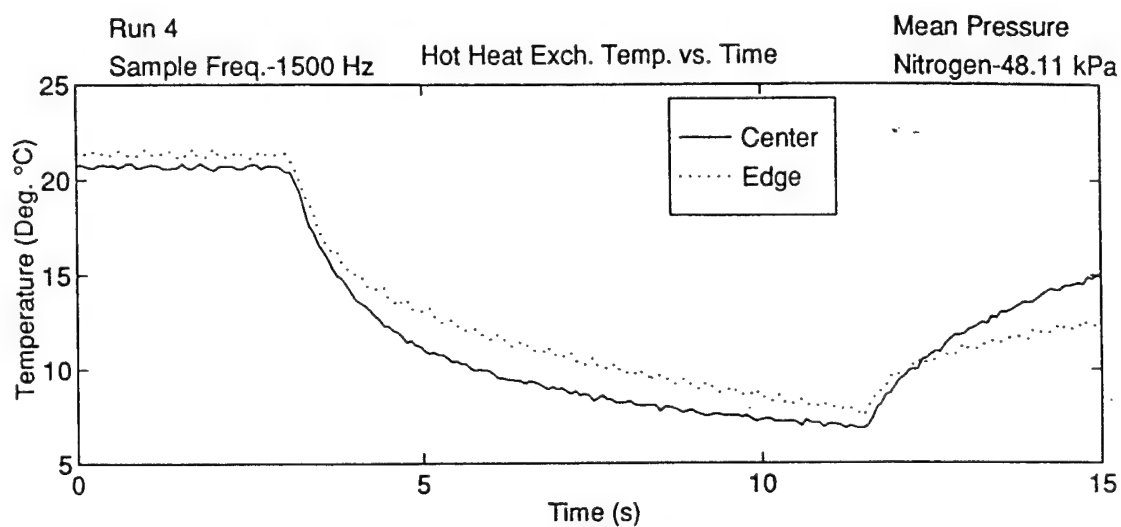
The measurements reported in this thesis point to a problem with the thermal contact of the heat exchanger fins. The stack, originally designed for a different purpose, was also prone to gas leaks. The two problems are related. It is recommended that a new stack be built, specifically designed for this project.

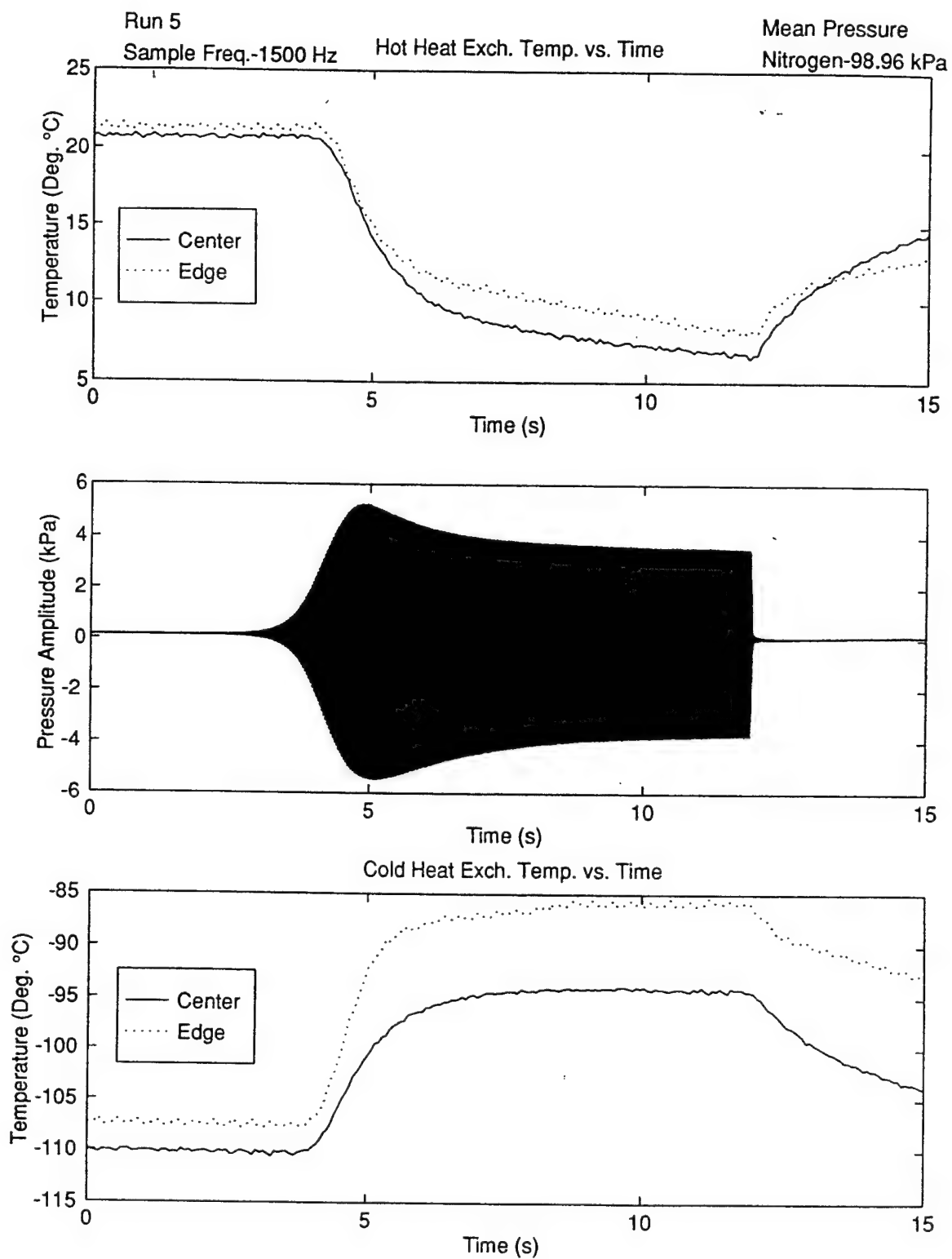


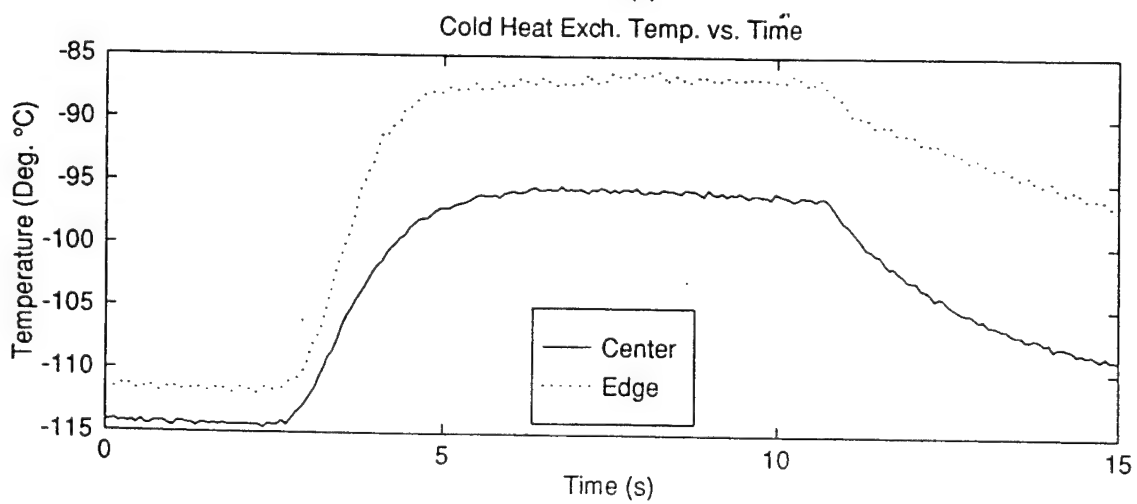
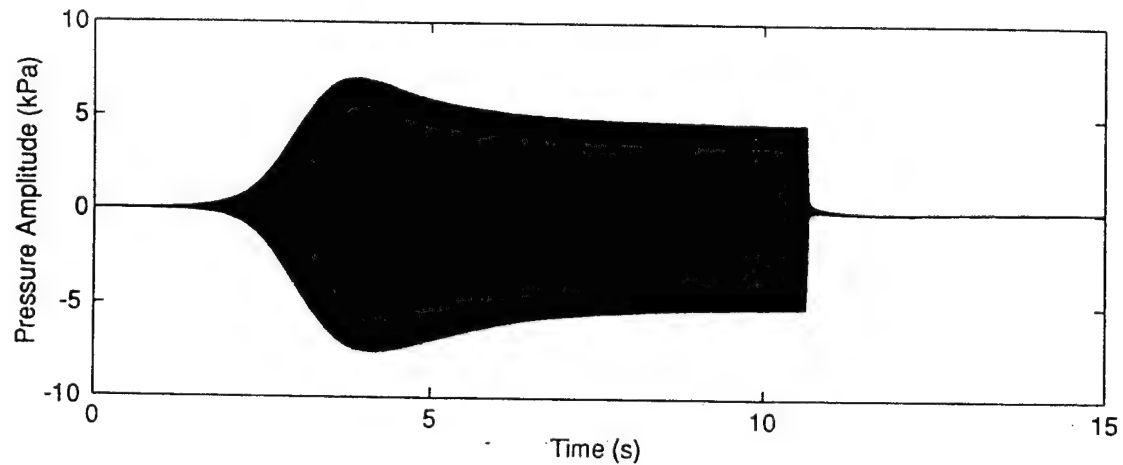
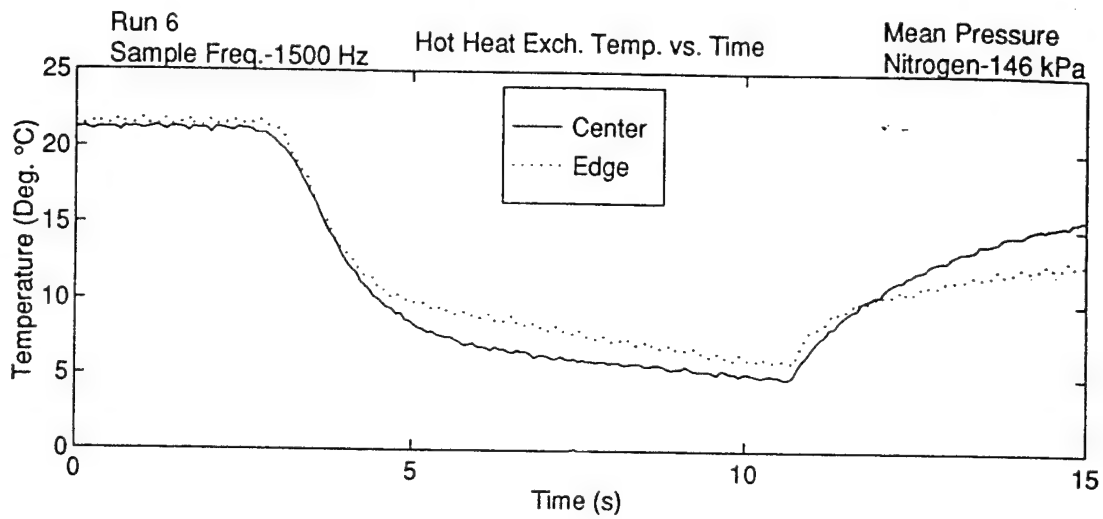
## APPENDIX A. GRAPHS OF EXPERIMENTAL RESULTS



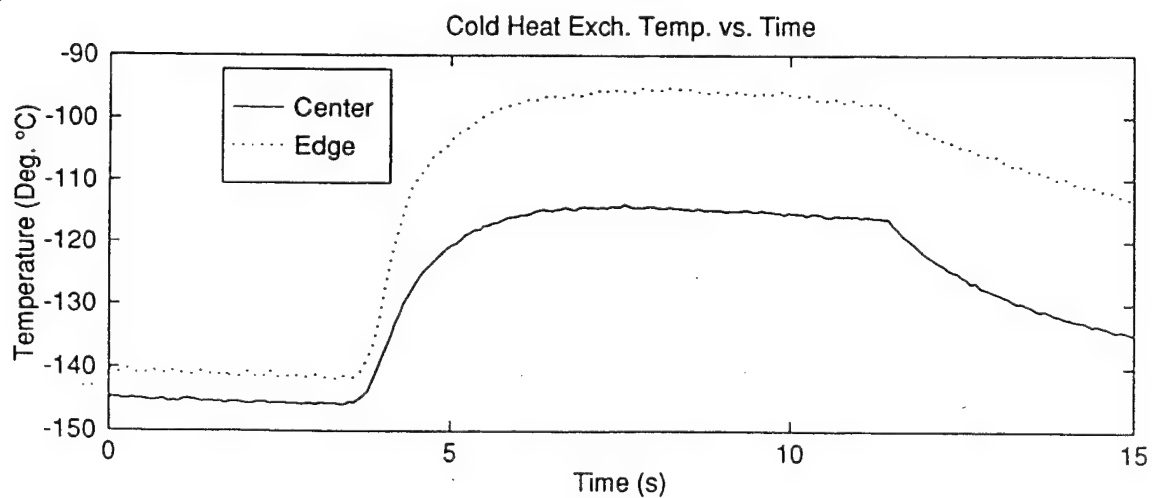
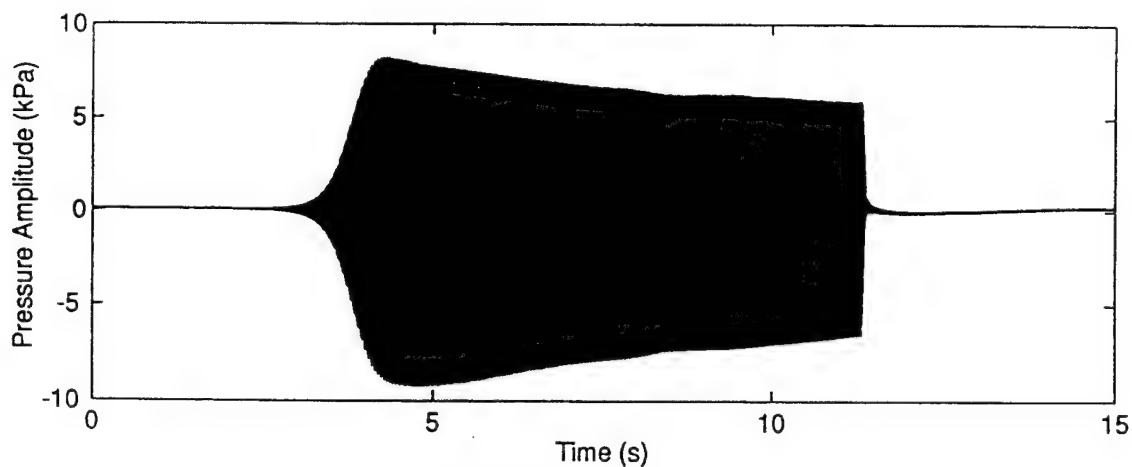
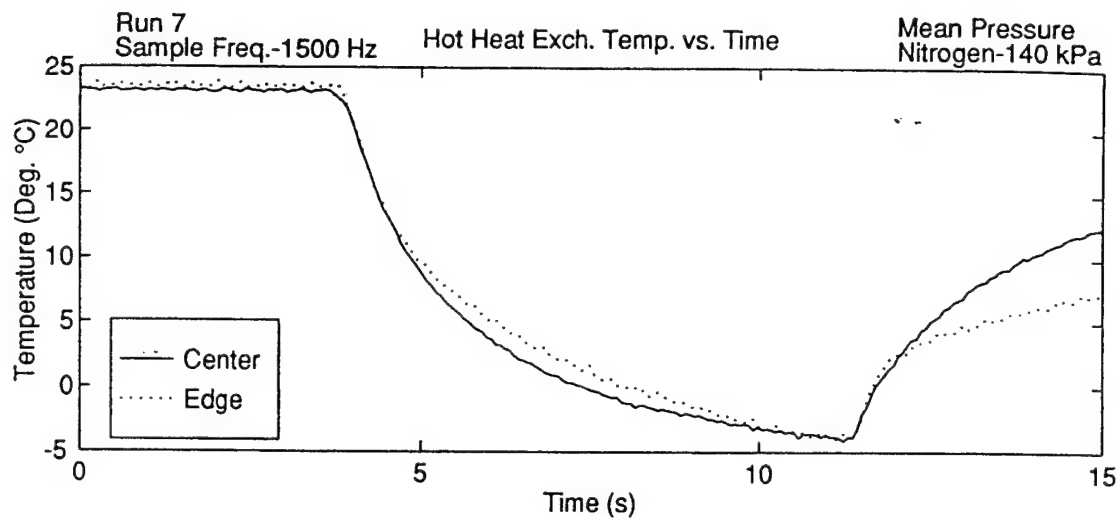


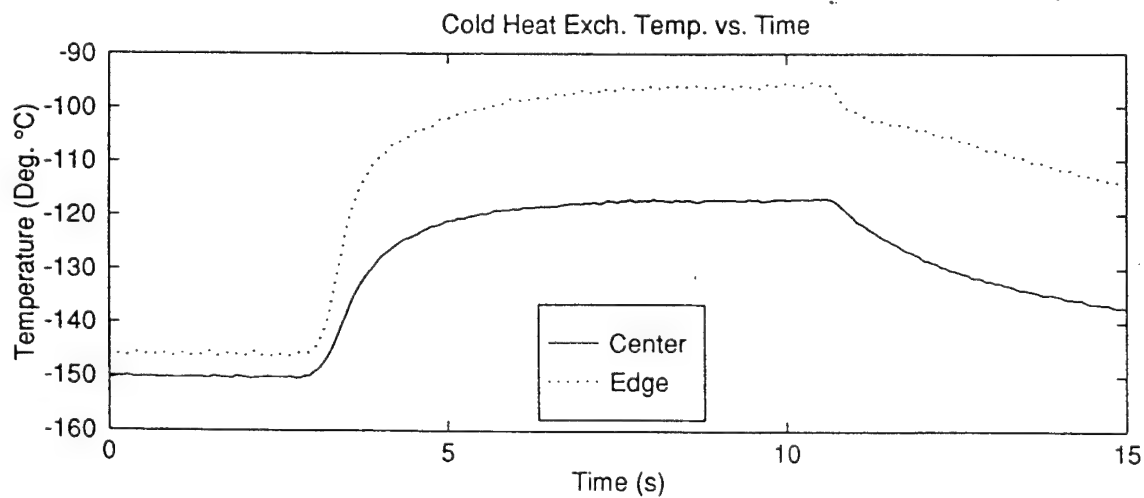
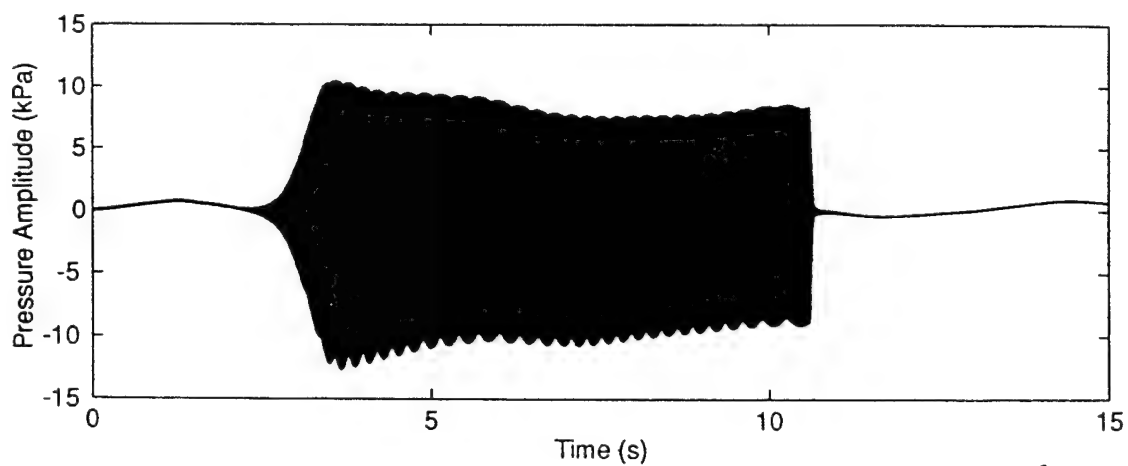
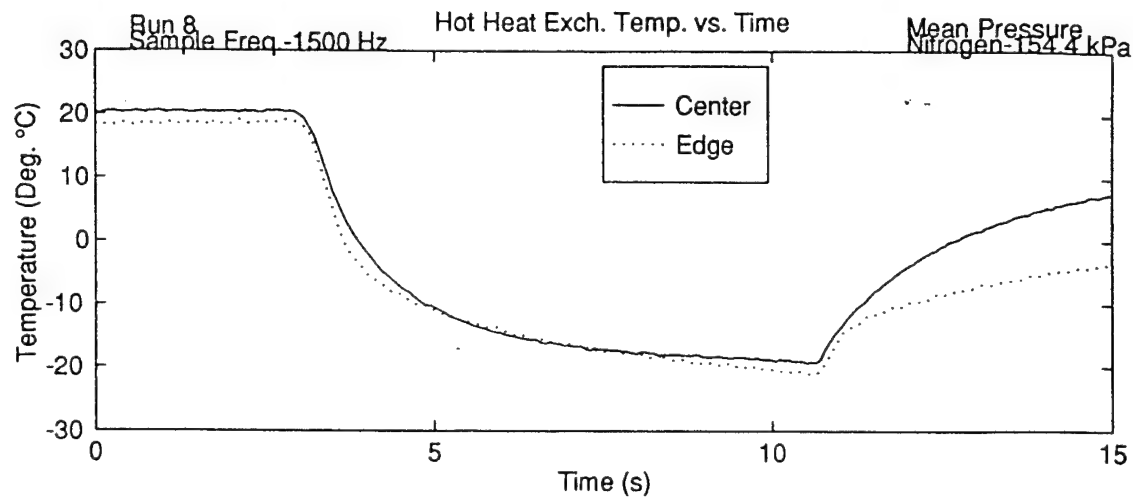


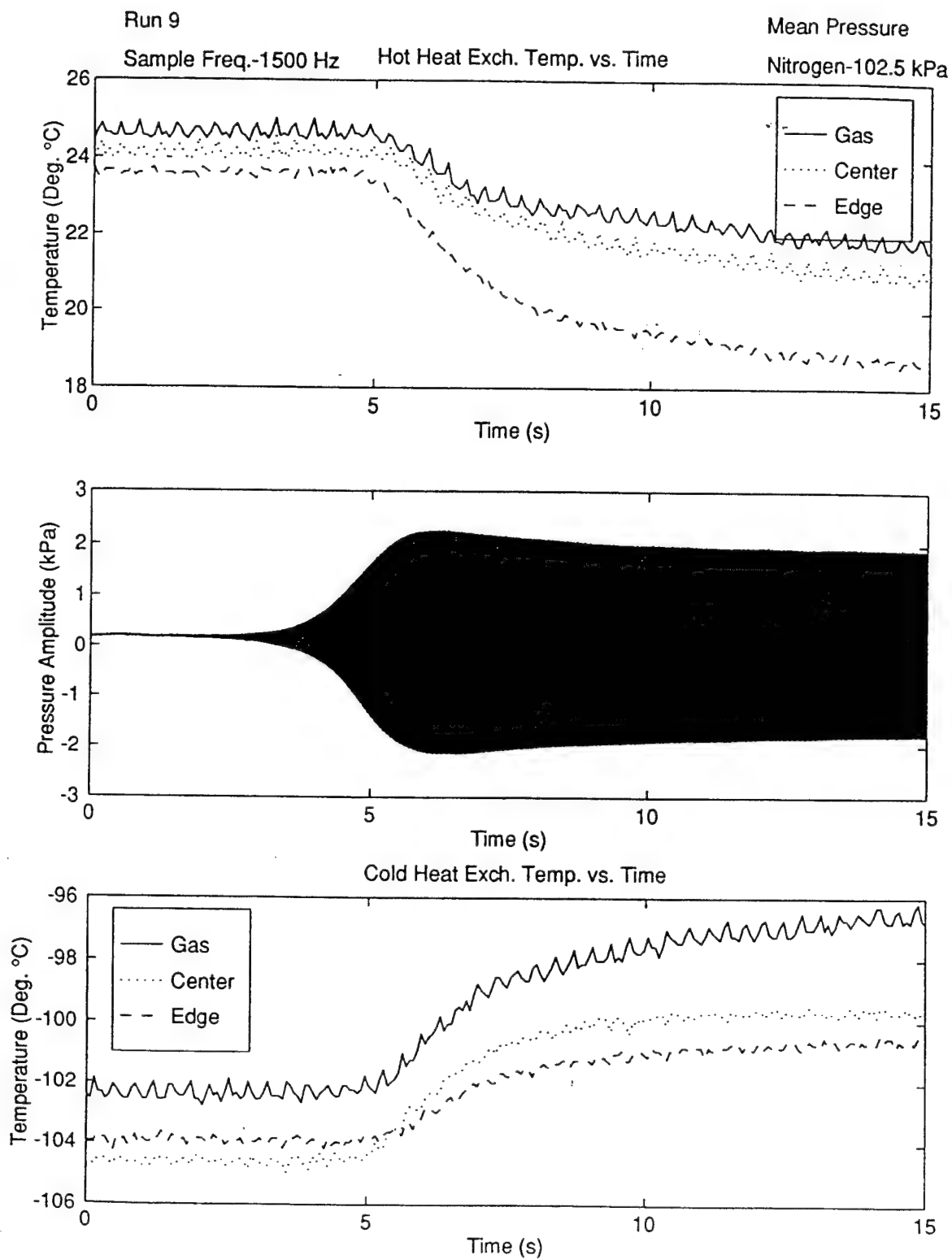


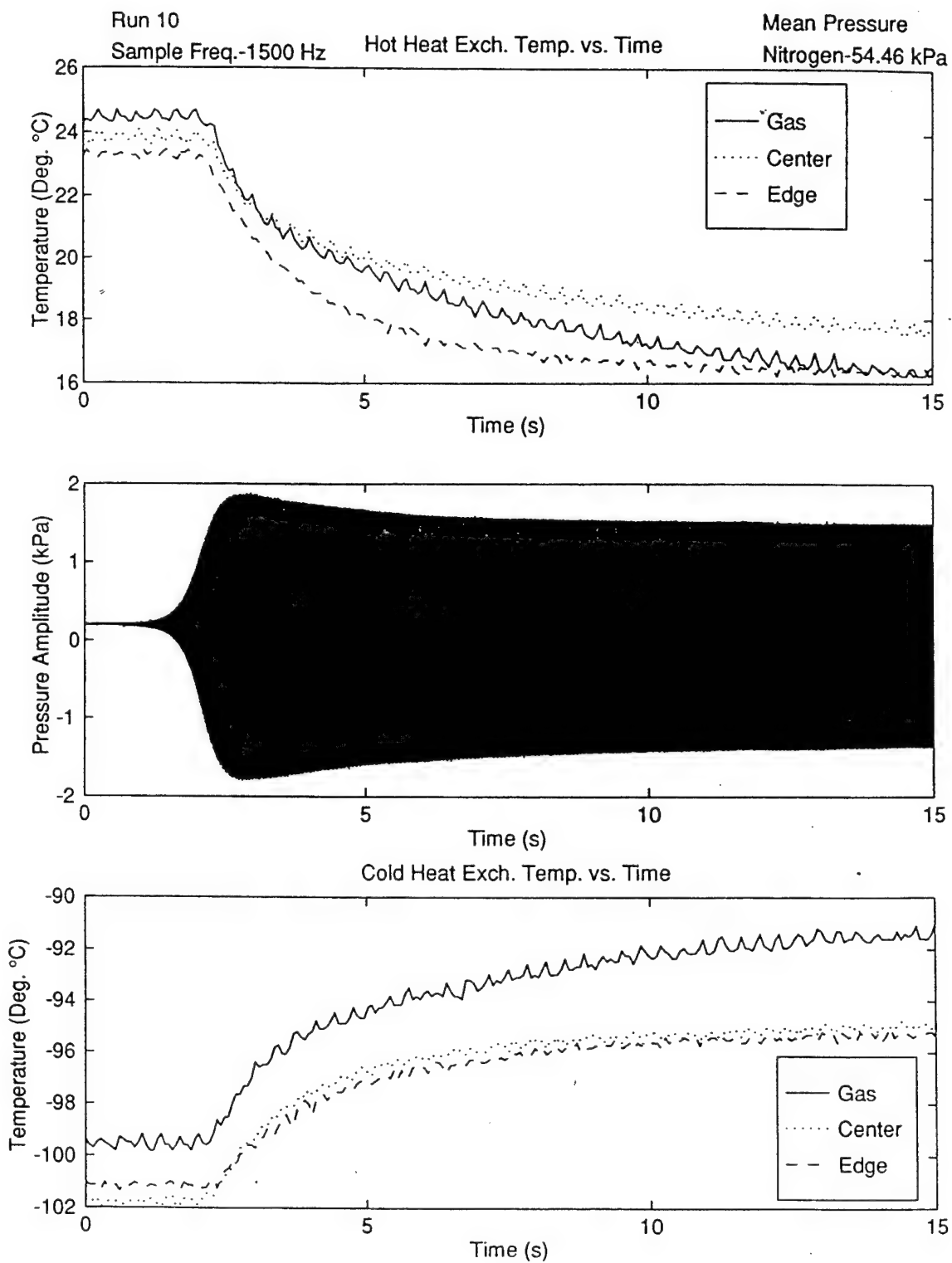


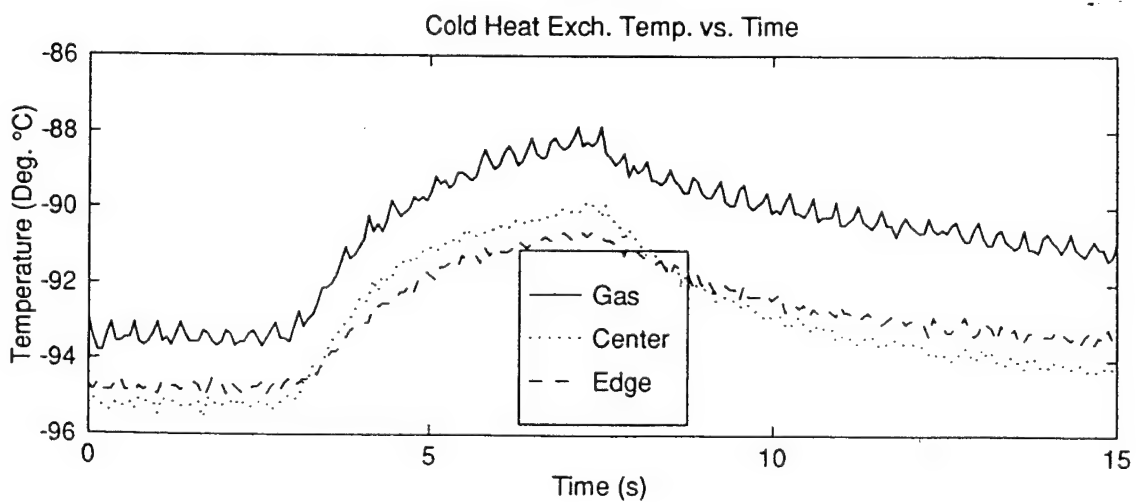
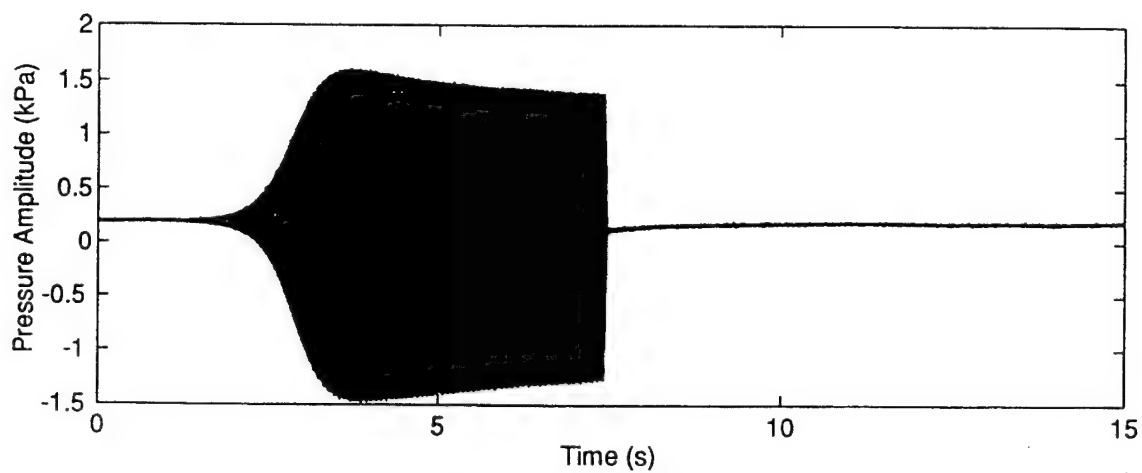
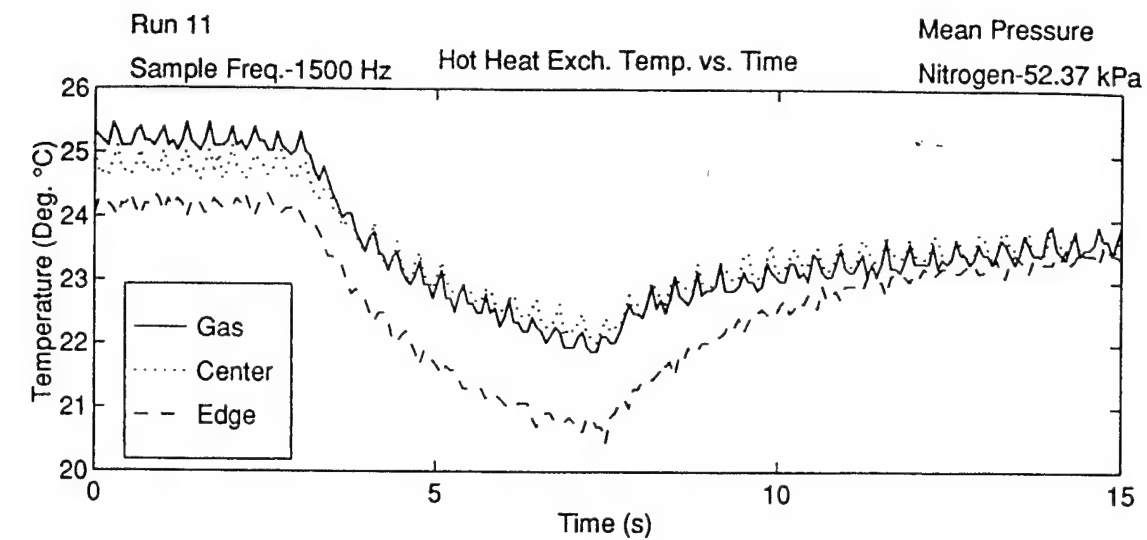


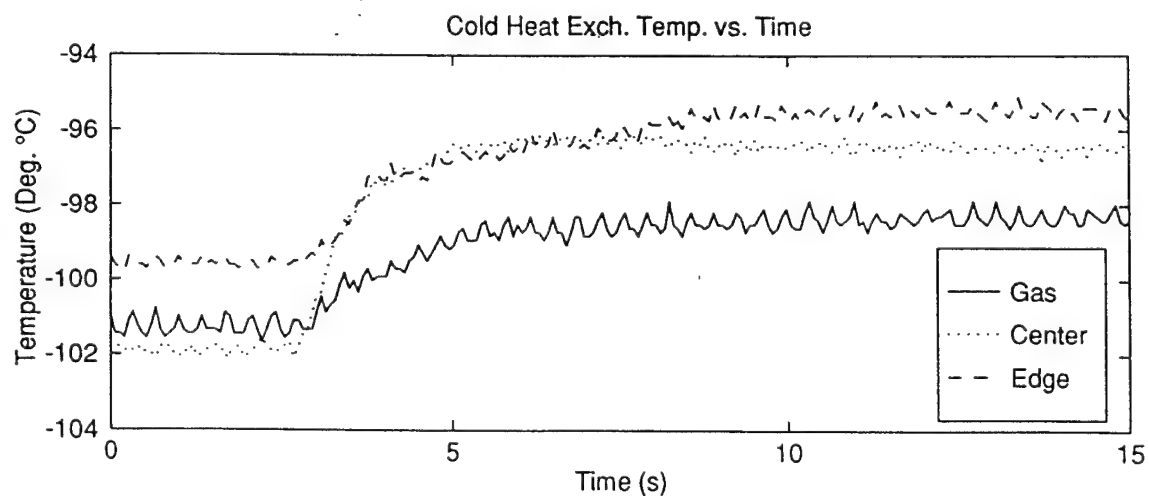
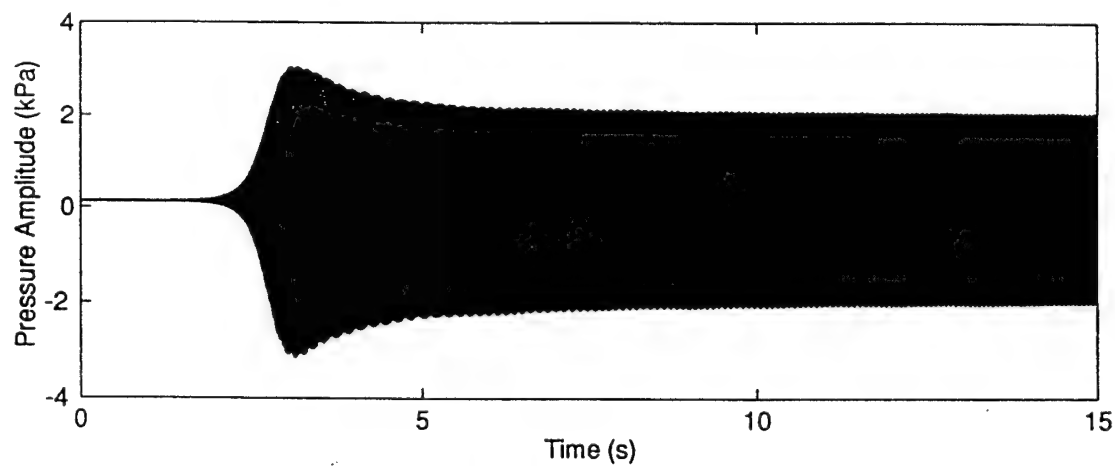
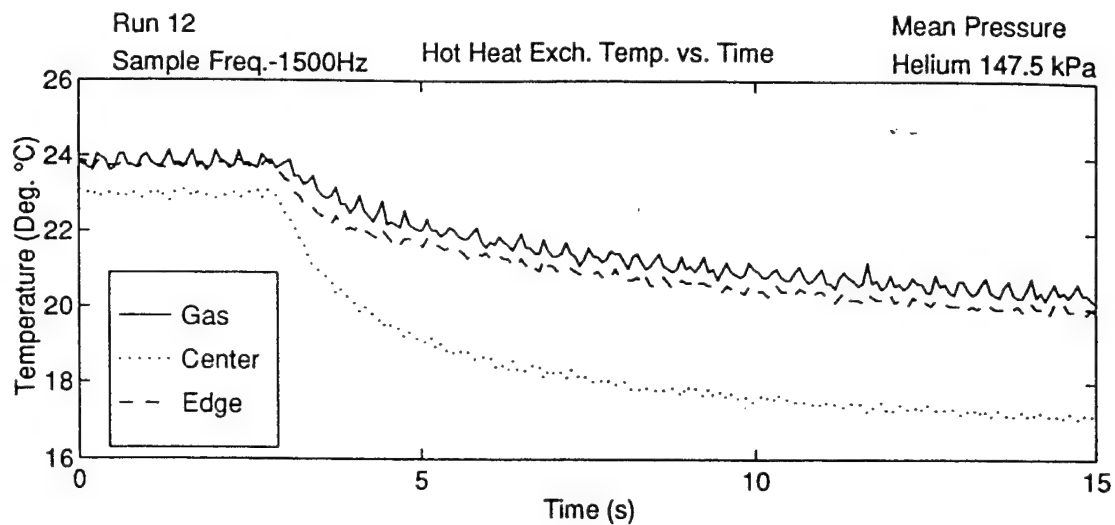


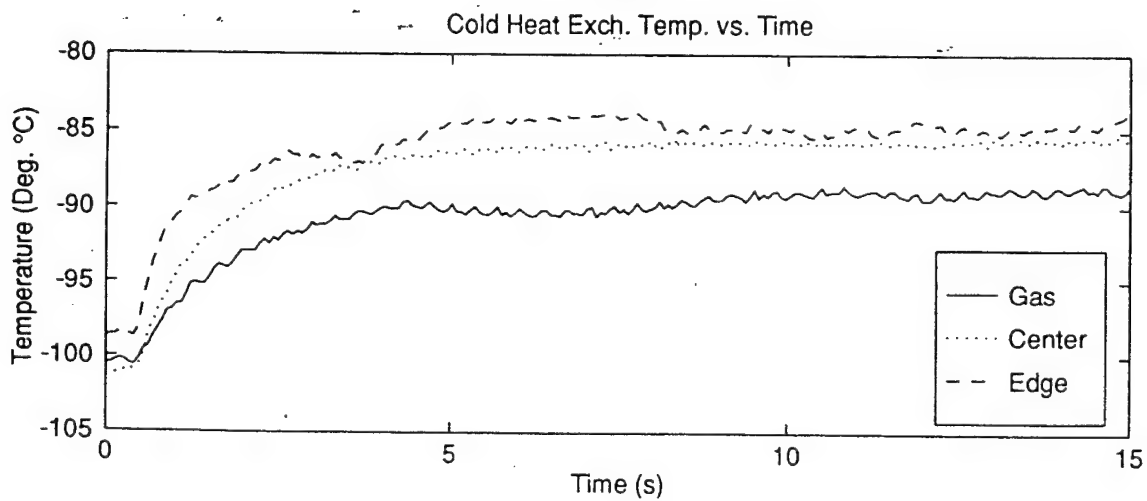
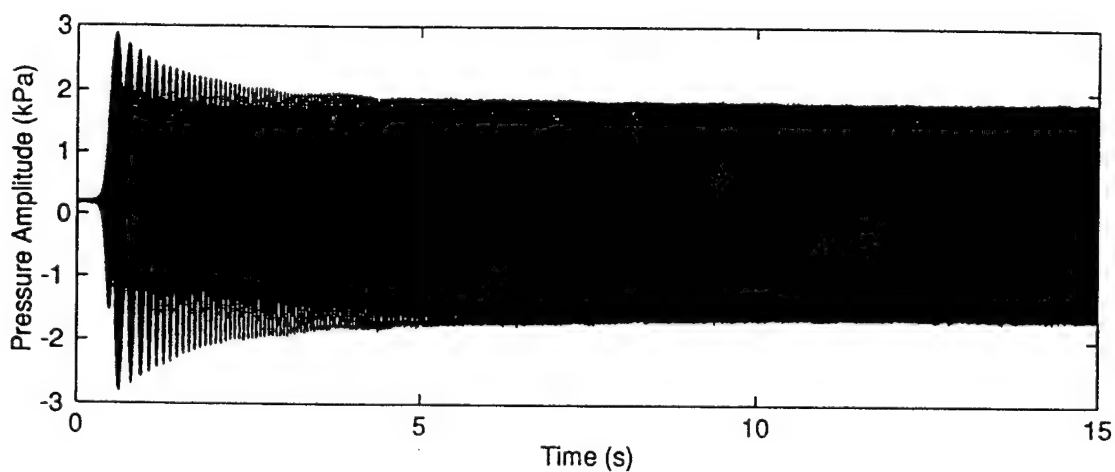
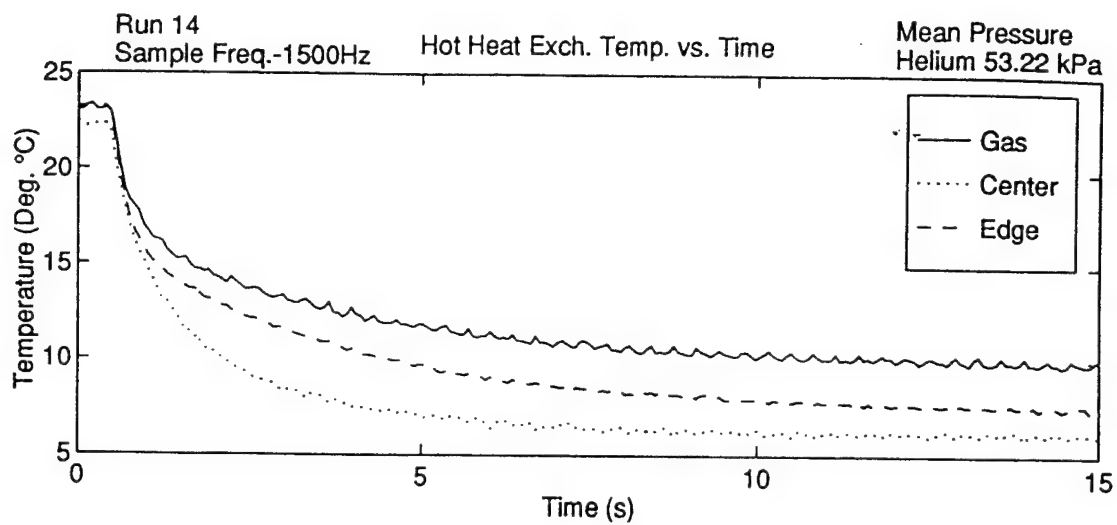


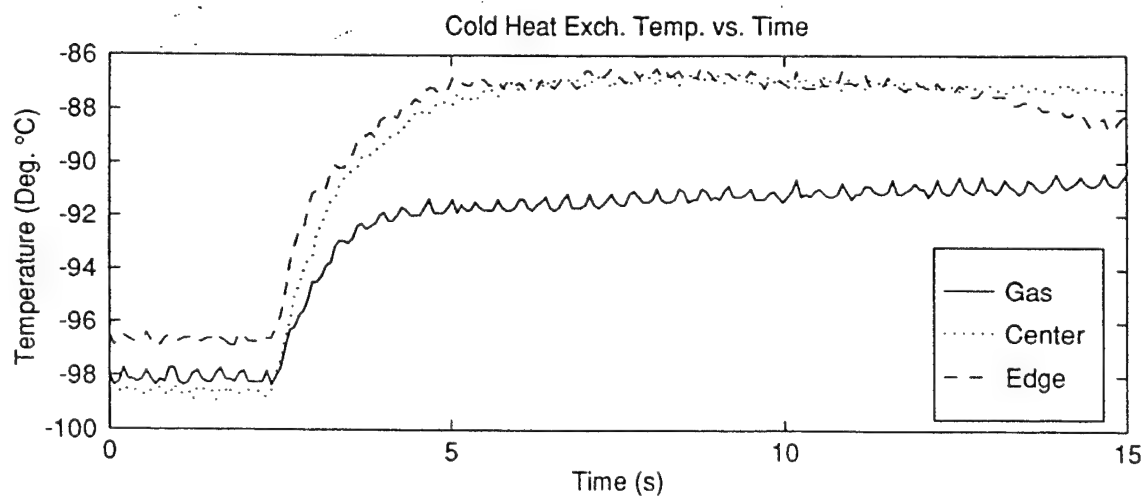
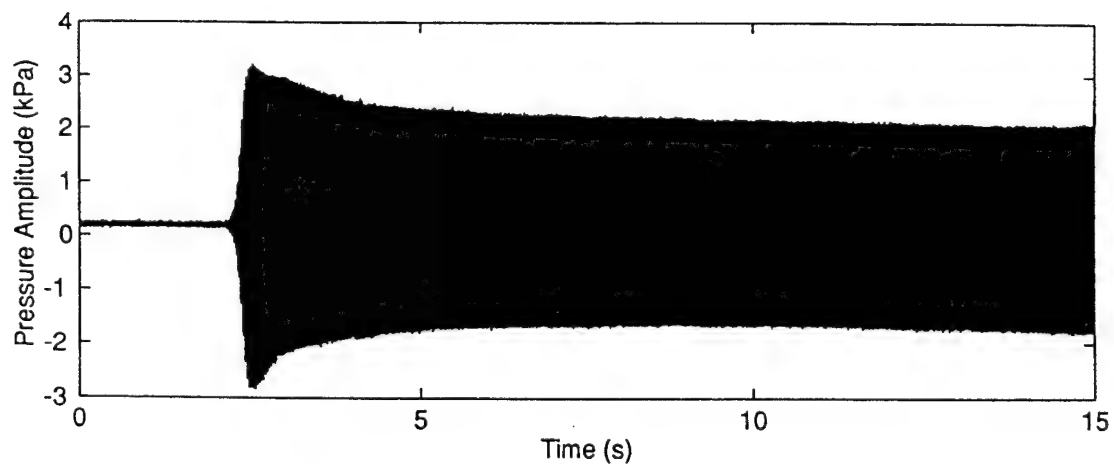
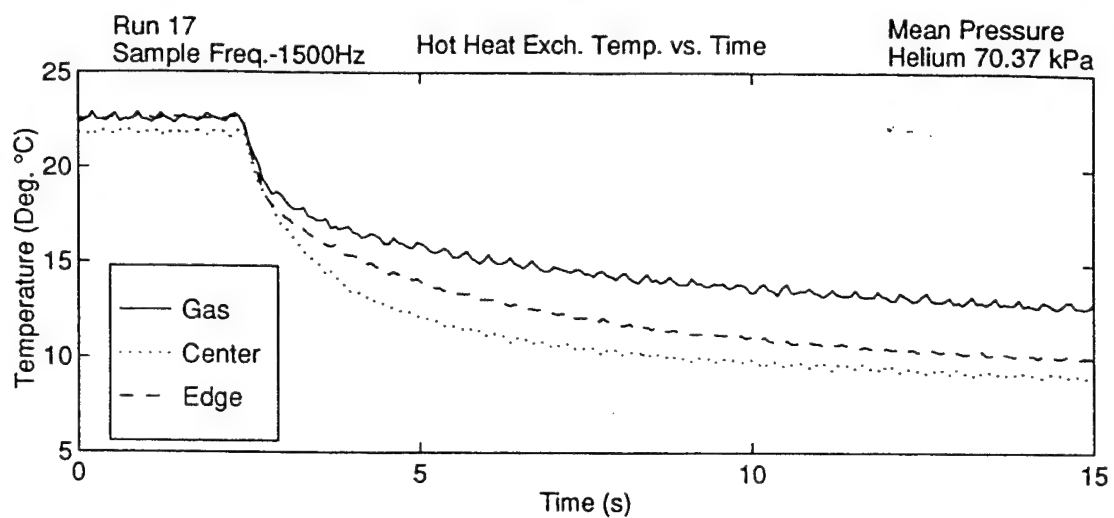




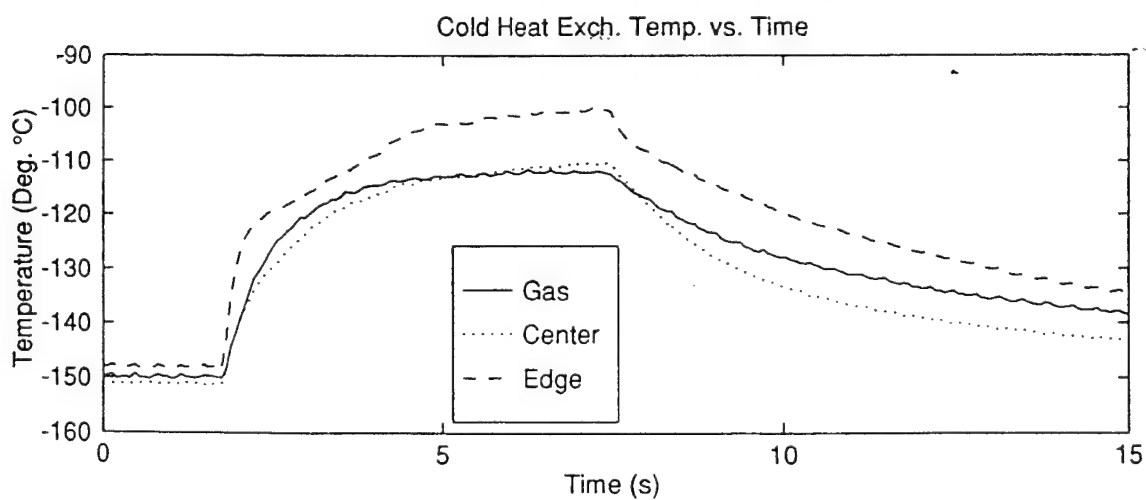
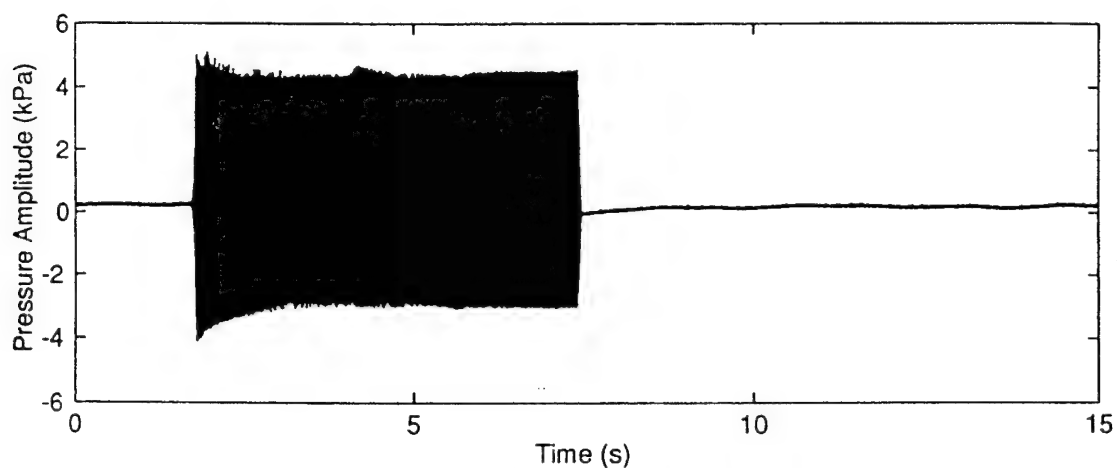
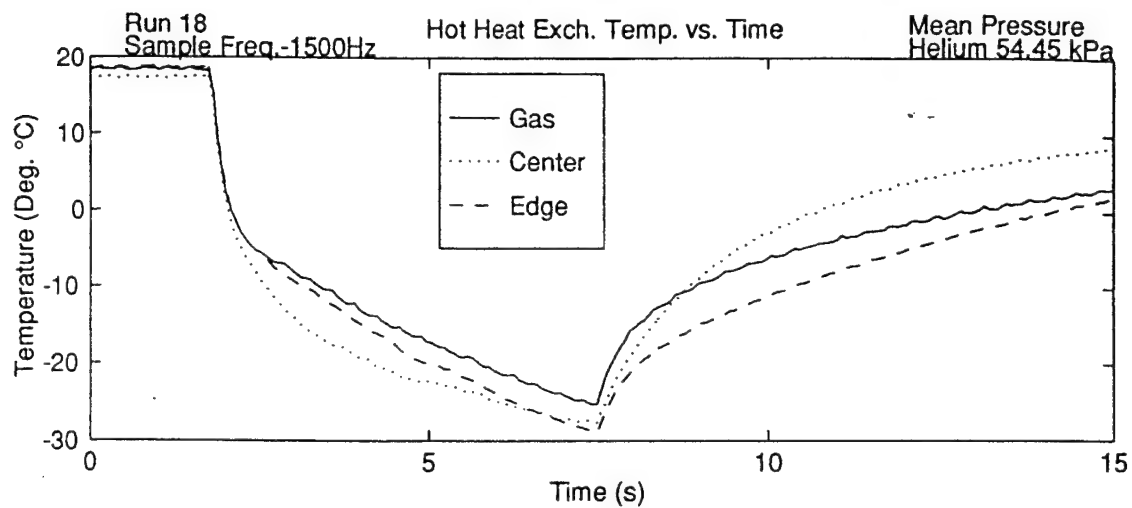


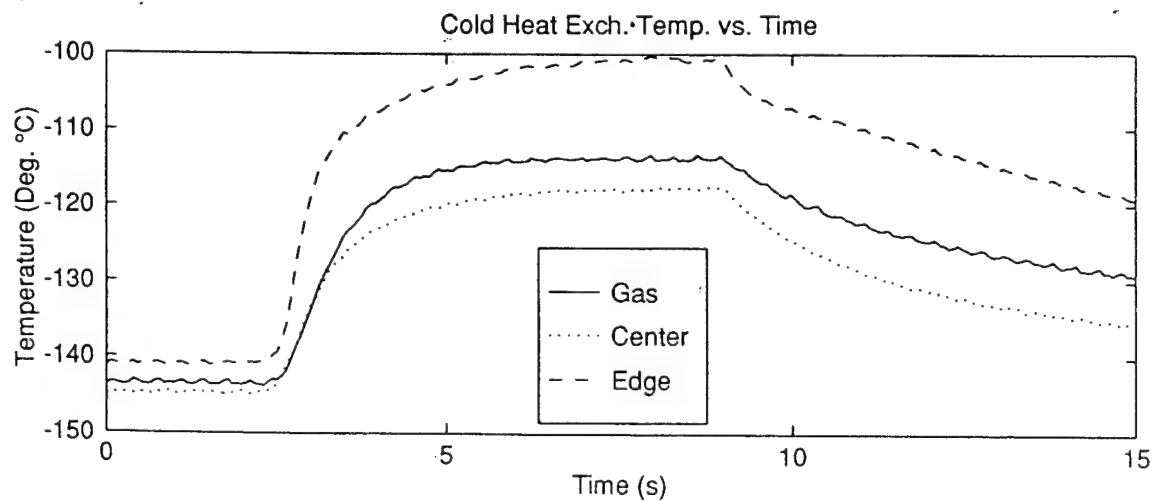
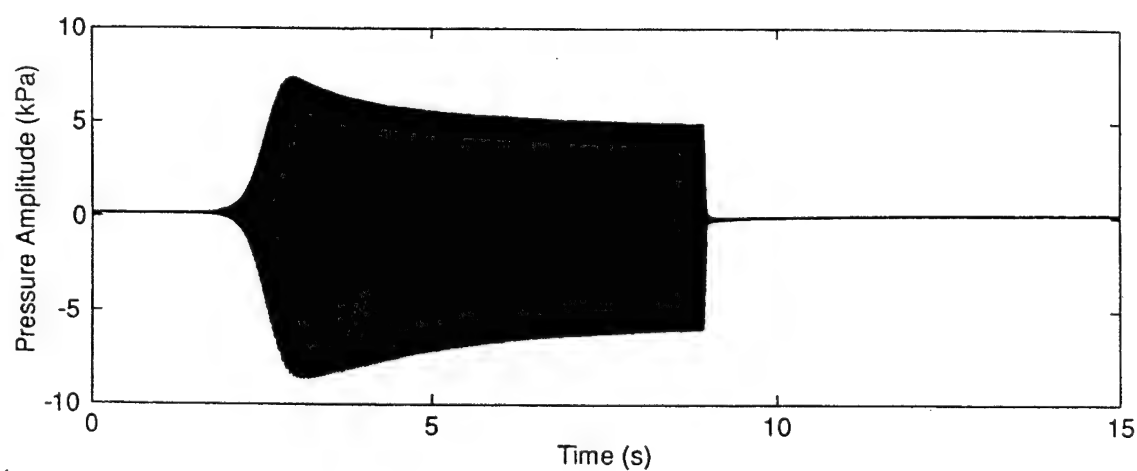
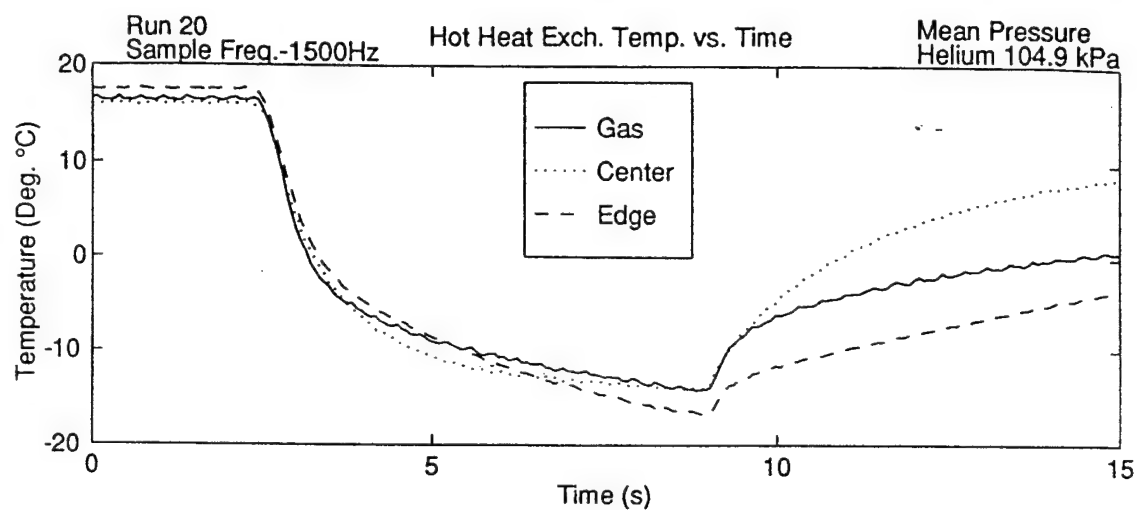


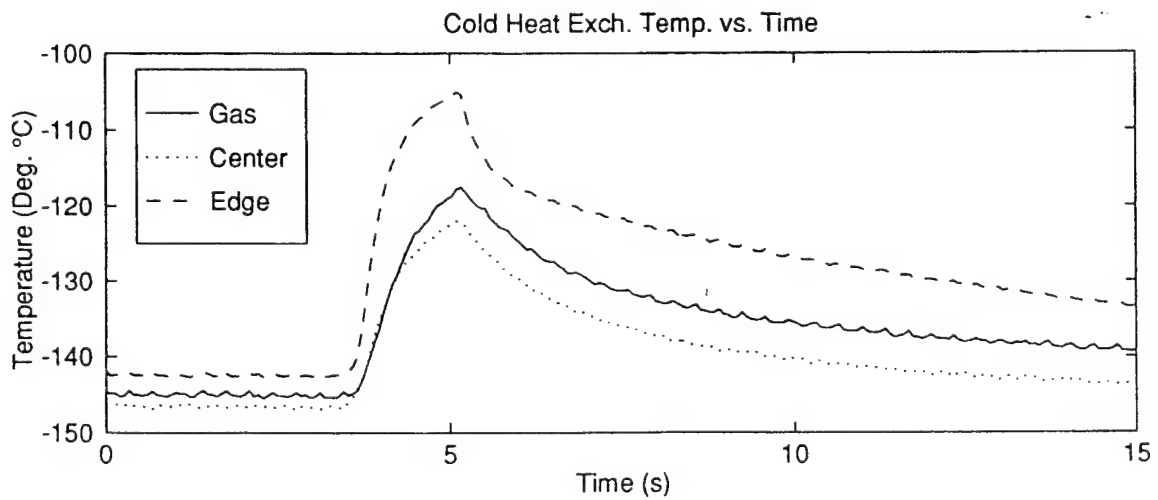
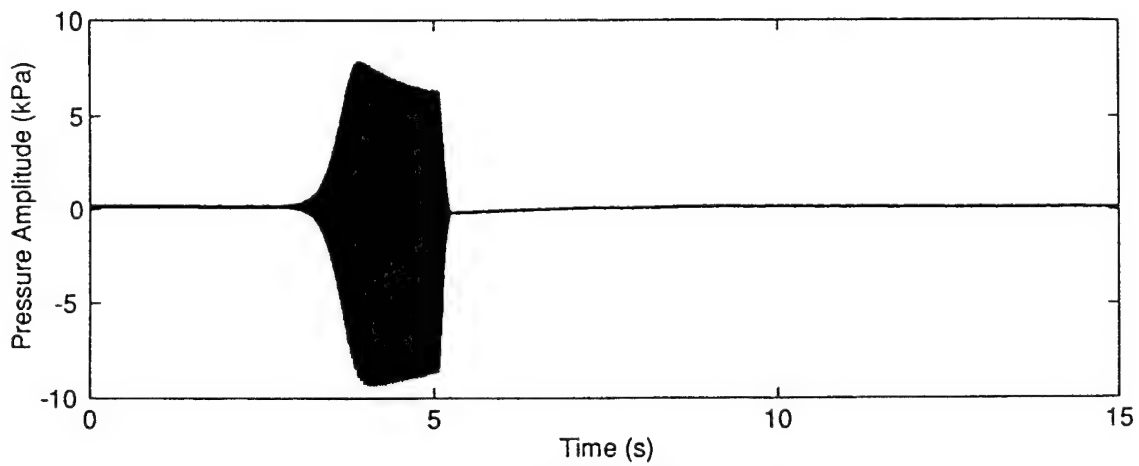
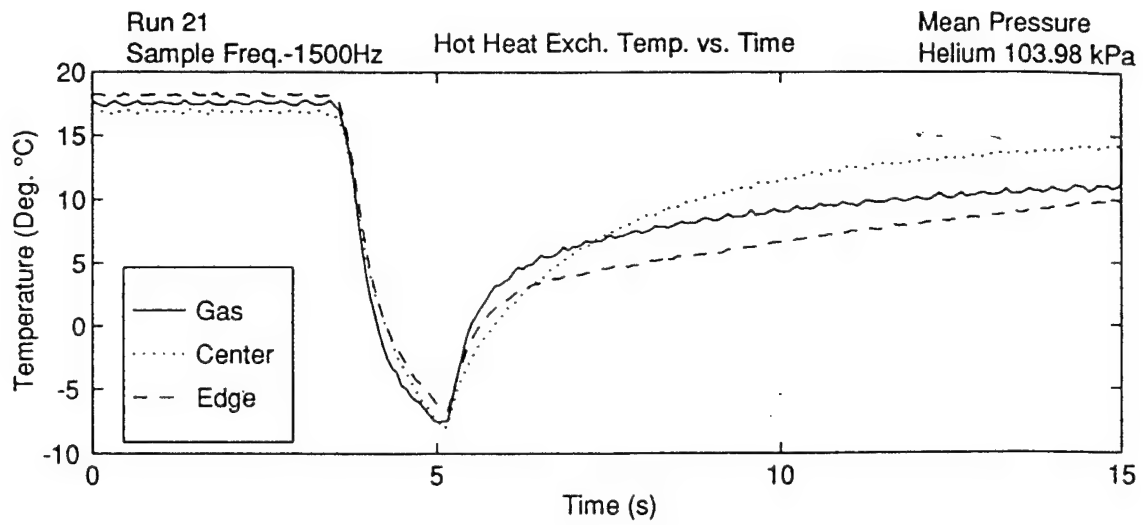












## APPENDIX B. TEMPERATURE PROFILES

Temperature File (° C)

Channel	Run2 Start	Run 2 End	Run3Start	Run 3 End	Run4 Start	Run 4 End
Ref. Temp	38.1	38.1	38.1	38.1	38.1	38.1
Cold Cap	-154.4	-154.8	-136.7	-136.7	-154.4	-154.8
Cold Center	-148.3	-147.1	-136.3	-137.9	-148.3	-147.1
Cold flange	-124.9	-120.5	-102.8	-103.5	-124.9	-120.5
C-Exch gas	-117.6	-111.2	-94.8	-94.5	-117.6	-111.2
C-Exch cen	-120	-115.2	-97	-98	-120	-115.2
C-Exch edge	-119.7	-113.6	-96.8	-96.6	-119.7	-113.6
H-Exch gas	22.6	19	22.9	19.9	22.6	19
H-Exch cen	21.8	20.5	21.7	20.4	21.8	20.5
H-Exch edge	22.3	17.6	22.4	19.4	22.3	17.6
Hot Flange	22.9	23	23	22.4	22.9	23
Hot Cap	23.2	23.1	23.9	24	23.2	23.1

Temperature File (° C)

Channel	Run5 Start	Run 5 End	Run 6 Start	Run 6 End	Run7 Start	Run 7 End
Ref. Temp	38.1	38.1	38.1	38.1	38	38
Cold Cap	-147	-148.7	-148.7	-154.5	-167.8	-173.6
Cold Center	-151.5	-153.4	-153.4	-157.5	-188.3	-189.2
Cold flange	-115	-116.5	-116.5	-121.9	-154.4	-154.2
C-Exch gas	-106.7	-105	-105	-109.7	-139.2	-136.9
C-Exch cen	-109.2	-109.8	-109.8	-114.7	-143.4	-143.4
C-Exch edge	-108.6	-107.7	-107.7	-112.6	-141.9	-140.3
H-Exch gas	21.9	18.1	18.1	18.6	24.1	17.6
H-Exch cen	21.1	19.7	19.7	20.2	23.5	21.1
H-Exch edge	21.7	17.6	17.6	17.7	23.8	17
Hot Flange	22.4	22.3	22.3	22.5	24.1	23.9
Hot Cap	23.8	23.9	23.9	23.7	23.4	24

Temperature File (° C)

Channel	Run8 Start	Run 8 End	Run9 Start	Run 9 End	Run10Start	Run10 End
Ref. Temp	38	38	32.8	32.8	32.8	32.8
Cold Cap	-187.5	-187.8	-79.8	-79.8	-82.6	-83.3
Cold Center	-174.7	-179.4	-93	-93.1	-92.5	-92.3
Cold flange	-161.1	-156.1	-109.1	-108.7	-105.7	-104.3
C-Exch gas	-149.5	-139.6	-102.2	-100.4	-99.4	-96.3
C-Exch cen	-153.7	-146.7	-104.4	-103.6	-101.5	-99.3
C-Exch edge	-153	-143	-103.8	-102.6	-100.9	-98.2
H-Exch gas	21.8	11.9	24.6	23.6	24.5	21.5
H-Exch cen	19.9	18	23.7	23.1	23.4	22.2
H-Exch edge	20.7	9.9	24	22.9	23.8	20.9
Hot Flange	23.7	22.1	25.1	25.3	25.1	24.8
Hot Cap	24.1	24.1	24	24.4	24.1	24

Temperature File (° C)

Channel	Run11Start	Run11End	Run12Start	Run12End	Run13Start	Run13 End
Ref. Temp	32.9	32.9	33.5	33.5	33.6	33.6
Cold Cap	-84.6	-85.5	-96	-95.8	-96.6	-96.7
Cold Center	-91.8	-91.7	-100.9	-100.9	-100.8	-100.6
Cold flange	-99.5	-98.4	-106.7	-105.6	-105.7	-102.8
C-Exch gas	-93.6	-96	-99.4	-96.5	-98.5	-88.1
C-Exch cen	-95.3	-96.7	-101.7	-99	-100.8	-91.3
C-Exch edge	-94.7	-95.9	-101.3	-98.8	-100.3	-91.1
H-Exch gas	25.2	23.2	23.9	20.6	23.4	11.7
H-Exch cen	24.3	22.1	23.2	19.5	22.4	13.3
H-Exch edge	24.9	22.9	23.9	20.8	23.1	13.4
Hot Flange	25.4	25.2	25.3	24.5	24.6	23.3
Hot Cap	24.3	23.9	24	24.3	23.7	23.9

Temperature File (° C)

Channel	Run17 Start	Run17 End	Run18Start	Run18 End	Run20Start	Run20 End
Ref. Temp	33.6	33.6	33.6	33.6	33.5	33.5
Cold Cap	-96.4	-95.4	-162.9	-161.8	-151.3	-151.5
Cold Center	-99.9	-99.8	-167.2	-165.6	-152.9	-152.6
Cold flange	-103.5	-102	-159.9	-157.5	-150.9	-147.8
C-Exch gas	-96.4	-94.3	-147.5	-147.3	-140.9	-136
C-Exch cen	-98.2	-96.6	-150.5	-150.8	-144.6	-140.3
C-Exch edge	-97.9	-95.9	-149.5	-149.7	-143.5	-138.1
H-Exch gas	22.7	19.3	19	15.7	17.5	13.6
H-Exch cen	21.9	19.6	17.6	14.4	16	14.7
H-Exch edge	22.5	19.3	18.6	14.7	16.4	10.9
Hot Flange	23.5	23	19.7	18.3	18	18
Hot Cap	23.1	23.7	22.7	22.7	20.2	20.3



Temperature File (° C)

Channel	Run21 Start	Run21 End				
Ref. Temp	33.5	33.5				
Cold Cap	-148.4	-148.4				
Cold Center	-147.9	-149.1				
Cold flange	-153.6	-155.7				
C-Exch gas	-142.1	-142.4				
C-Exch cen	-146.1	-146.9				
C-Exch edge	-144.6	-144.8				
H-Exch gas	18.1	16.5				
H-Exch cen	16.9	16.4				
H-Exch edge	17.5	14.9				
Hot Flange	18.7	19				
Hot Cap	19.9	19.9				

## APPENDIX C. DELTAE INPUT FILE FOR PRIME MOVER DESIGN

TITLE Meng prime mover

BEGIN Initial 0  
 0.52E+05 a Mean P Pa  
 200. b Freq. Hz  
 293 c T-beg K  
 5E+03 d  $l_{pl}@0$  Pa G  
 0.000 e  $Ph(p)0$  deg G  
 0.000 f  $l|U|@0$   $m^3/s$   
 0.000 g  $Ph(U)0$  deg  
 nitrogen Gas type  
 copper Solid type

ENDCAP Hot End 1  
 8.24E-04 a Area  $m^2$   
 sameas 0 Gas type  
 copper Solid type

ISODUCT Hot Duct 2  
 sameas 1a a Area  $m^2$   
 0.102 b Perim m  
 0.13 c Length m

sameas 0 Gas type  
 copper Solid type

HXFRST Hot HX 3  
 9.07E-04 a Area  $m^2$   
 0.62 b GasA/A  
 1.6E-03 c Length m  
 3.1E-04 d  $y_0$  m

20 e HeatIn W  
 293 f Est-T K (t)  
 sameas 0 Gas type  
 copper Solid type

STKSLAB Prime Mover Stack 4  
 sameas 3a a Area  $m^2$   
 0.62 b GasA/A  
 16.5E-03 c Length m  
 3.1E-04 d y0 m  
 0.19E-03 eLplate m  
 sameas 0 Gas type  
 kapton Solid type

HXLAST Ambient HX 5  
 sameas 3a a Area  $m^2$   
 0.62 b GasA/A  
 1.6E-03 c Length m  
 3.1E-04 d y0 m  
 0 e HeatIn W  
 120 f Est-T K  
 sameas 0 Gas type  
 copper Solid type

ISODUCT Cold Duct 6  
 sameas 1a a Area  $m^2$   
 0.102 b Perim m  
 0.55 c Length m  
 sameas 0 Gas type  
 copper Solid type

ENDCAP Cold End 7  
 sameas 1a a area  
 sameas 0 Gas type  
 copper solid type

HARDEND 8 8

0.000 a R(1/Z)

0.000 b I(1/Z)

sameas 0 gas type

copper solid type



## LIST OF REFERENCES

1. G. W. Swift, "Thermoacoustic Engines," J. Acoust. Soc. Am. Vol. 84, 1145-1180 (1988).
2. Anthony A. Atchley, "Standing Wave Analysis of a Thermoacoustic Prime Mover Below Onset of Self-Oscillation," J. Acoust. Soc. Am. 92(5), 2907-2914(1992).
3. John Wheatley, T. Hofler, G. W. Swift and A. Migliori, "An Intrinsically Irreversible Thermoacoustic Heat Engine," J. Acoust. Soc. Am. Vol 74, 153-170 (1983).
4. Anthony A. Atchley et. al., "Study of a Thermoacoustic Prime Mover Below Onset of Self-Oscillation," J. Acoust. Soc. Am. 91(2), 734-743 (1992).
5. Fan-Ming, Kuo, "Stability Curves for a Thermoacoustic Prime Mover," Master's Thesis, Naval Postgraduate School, California June 1993.
6. A. Prosperetti and H. Yuan, "A simplified model of a thermoacoustic refrigerator." J. Acoust. Soc. Am. Vol 98, No. 5, Pt. 2, 2961(A), 1995.
7. John Wheatley, T. Hofler, G. W. Swift and A. Migliori, "Understanding Some Simple Phenomena In Thermoacoustics With Applications To Acoustical Heat Engines," Am. J. Phys. 53, 147-162 (1985).
8. W. C. Ward, G. W. Swift, Design Enviroment for Linear Thermoacoustic Engine DELTAE Tutorial and user's Guide, Los Alamos National Laboratory, July 1993.



## INITIAL DISTRIBUTION LIST

	No. Copies
1. Defense Technical Information Center 8725 John J. Kingman Rd. , STE 0944 Ft. Belvoir, VA 22060-6218	2
2. Dudley Knox Library Naval Postgraduate School 411 Dyer Rd. Monterey, CA 93943-5101	2
3. Prof. Anthony A. Atchley, Code PH/Ay Department of Physics Naval Postgraduate School Monterey, CA 93943	4
4. Prof. Robert M. Keolian, Code PH/Kn Department of Physics Naval Postgraduate School Monterey, CA 93943	1
5. Major Lin, Hsiao-Tseng SGC # 2552, Naval Postgraduate School Monterey, CA, 93943	1
6. LT. Chuang, Ming-Fei SGC # 2552, Naval Postgraduate School Monterey, CA, 93943	1
7. LCDR. Meng, Ching-Kai 2F #1 lane 60 Ning An St. Taipei, Taiwan R.O.C.	1